Terrace stratigraphy, ages, and incision rates along the Rio Ojo Caliente, north-central New Mexico

Daniel J. Koning, Dennis L. Newell, Andrei Sarna-Wojcicki, Nelia Dunbar, Karl Karlstrom, Anthony Salem, and Laura Crossey, 2011, pp. 281-300

in:

Geology of the Tusas Mountains and Ojo Caliente, Author Koning, Daniel J.; Karlstrom, Karl E.; Kelley, Shari A.; Lueth, Virgil W.; Aby, Scott B., New Mexico Geological Society 62nd Annual Fall Field Conference Guidebook, 418 p.

This page is intentionally left blank to maintain order of facing pages.

New Mexico Geological Society Guidebook, 62nd Field Conference, Geology of the Tusas Mountains - Ojo Caliente, 2011, p. 281-300.

TERRACE STRATIGRAPHY, AGES, AND INCISION RATES ALONG THE RIO OJO CALIENTE, NORTH-CENTRAL NEW MEXICO

DANIEL J. KONING[1], DENNIS L. NEWELL[2], ANDREI SARNA-WOJCICKI[3], NELIA DUNBAR[1], KARL KARLSTROM[4], ANTHONY SALEM[4], AND LAURA CROSSEY[2]

[1] New Mexico Bureau of Geology and Mineral Resources, 801 Leroy Place, Socorro, NM 87801; dkoning@nmt.edu

[2]Los Alamos National Laboratory, Earth and Environmental Science Division (EES-14), MS J966, Los Alamos, NM 87545

[3]U.S. Geological Survey, 345 Middlefield Road, MS 975, Menlo Park, CA 94025

[4]Department of Earth and Planetary Science, University of New Mexico, Albuquerque, NM 87131

Abstract—We present new tephrochronologic and radiometric data that constrain the ages of terraces along the Rio Ojo Caliente. Draining the southern Tusas Mountains, the Rio Ojo Caliente is a tributary of the Rio Chama in the northwestern Española Basin. The highest terrace, labeled Qtoc1, has a strath located 107-134 m above the modern river. Qtoc1 contains ash and pumice-lapilli tephra probably correlative to the Guaje Pumice Bed of the Otowi Member of the Bandelier Tuff (1.61-1.63 Ma), although correlation to the Tsankawi Pumice Bed of the Tshirege Member of the Bandelier Tuff (1.22-1.26 Ma) is permissible. The second highest terrace, labeled Qtoc2, is 95-103 m above the modern river and correlates to terraces along the Rio Chama that contain the Lava Creek B ash (640 ka). The strath of the most laterally extensive terrace lies 19-30 m above the modern river. Called the 20-40 m terrace (labeled Qtoc6 in this study), it is older than 103 ka and probably younger than 210 ka based on stratigraphic relations and three U-series ages of an adjacent travertine mound complex. Both the Qtoc6 terrace and the next higher terrace level (Qtoc5) are characterized by having two straths (erosional terrace bases) separated by 2-7 m. Quartzite-rich gravel that overlies these strath couplets is generally 3-6 m-thick. Overlying these basal gravels is a 10-18 m-thick sequence of alluvium with higher sand content and higher amounts of locally derived alluvium. This sedimentologic trend indicates that following incision of the river to a new base level and deposition of axial gravel, subsequent aggradation was heavily influenced by input of detritus derived from nearby hillslopes and low order drainages; this locally derived alluvium was deposited as alluvial fans on the margins of the river valley. In the Holocene (present) interglacial, significant local erosion and aggradation has also occurred. Using this comparison, we agree with previous interpretations along the lower Rio Chama that locally derived, sand-dominated alluvium in the middle and upper parts of the terraces, best exposed in Qtoc6 and Qtoc5, were also deposited in interglacial climates or at the glacial/interglacial transition, and that strath formation and deposition of the quartzite-rich, basal gravel occurred largely during glacial climates (possibly at the glacial/interglacial transition). We use this process-response model to infer a preferred age of 130-160 ka for the Qtoc6 terrace deposit and its lowest strath. Consideration of terrace ages and their relative heights indicates an increase in incision rates after 640 ka, consistent with earlier interpretations.

INTRODUCTION

The Rio Ojo Caliente is a tributary of the lower Rio Chama that drains the southern Tusas Mountains (Fig. 1). Progressive incision along the Rio Ojo Caliente has resulted in impressive badlands that offer some of the best exposures of Quaternary terraces in the Española Basin. As part of a STATEMAP project, we mapped terraces for 35 km along the Rio Ojo Caliente, at a scale of 1:24,000, in four different quadrangles: Chili, Lyden, Ojo Caliente, and La Madera (Koning, 2004; Koning et al., 2005a and 2005b; Koning et al., 2007). In this paper, we synthesize this terrace mapping by comparing elevations of the base of the terraces (i.e., the terrace strath) as a function of distance for the entire river. Doing so allows us to compare the Rio Ojo Caliente terrace stratigraphy directly with lower Rio Chama terrace stratigraphy, similar to the approach of Newell et al. (2004). The Rio Chama has some of the best terrace age control in the southwest, which were obtained by a variety of geochronologic techniques that include radiocarbon dating, amino-acid racemization ratios, and chemical correlation of tephra beds (Dethier et al., 1990; Dethier and McCoy, 1993; Dethier and Reneau, 1995). Surface dating of Rio Chama terraces provides minimum ages for the underlying terrace deposit (Dethier et al., 1988).

Investigation of Quaternary deposits in the Española Basin and elsewhere in the southwestern United States has resulted in a climate-response geomorphic model for perennial river valleys in arid or semiarid environments (Hawley et al., 1976; Love et al., 1987; Bull, 1991; Dethier and Reneau, 1995; Rogers and Smartt, 1996), which is consistent with interpretations for ephemeral streams on the western margin of the Española Basin (Reneau et al., 1996a). In this paper, we argue that sedimentologic trends in the two best-exposed terraces support this model, which we will refer to as the "Southwest model." The Southwest model postulates that waxing periods of glacial climates correspond with episodes of increased river discharge and entrenchment along major river valleys. During full glacial climates in arid to semiarid environments in New Mexico, large portions of valley-border and piedmont slopes were stable because of relatively dense vegetative cover and weakened summer monsoonal circulation (Gutzler, 2004). During the transition from glaciations to inter-glaciations, decreased discharge along major rivers induced aggradation of valley bottoms. With an increase in aridity accompanying a transition to an interglacial climate, vegetation cover in lower elevations decreased and interglacial monsoonal precipitation events facilitated widespread erosion and sedimentation on valley borders. This local erosion and sedimentation promoted expansion of arroyo-mouth fans onto flood plains (Hawley et al., 1976).

The glacial-interglacial oscillations that are thought to drive alternating periods of aggradation and incision are superimposed on an overall trend of semi-steady bedrock incision that leaves the oldest terraces highest in the landscape and progressively

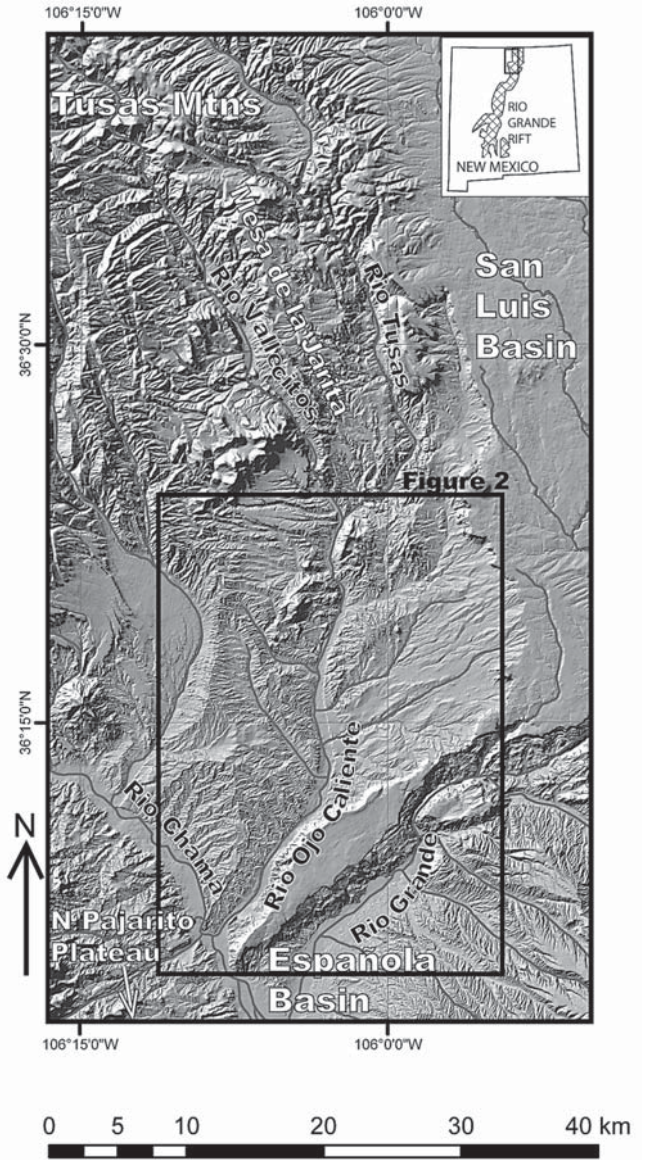

FIGURE 1. Shaded relief map showing the geographic context of the Rio Ojo Caliente. Rivers and major streams are shown in dark gray. Black rectangle shows the extent of the map in Figure 2.

younger river levels inset into older terraces. Across the erosional landscape of northern New Mexico, the Colorado Plateau, and the southern Rockies, long-term bedrock incision rates have averaged 50-160 m/Ma over the last several million years (e.g., Dethier et al., 1988; Dethier et al., 1990; Newell et al., 2004; Connell et al., 2005; Karlstrom et al., 2007; Aslan et al., 2010). There are three probable drivers for long term bedrock incision. The first is increased stream power linked to wetter climates after ~600 ka (Jansen et al., 1986; Sarnthein et al., 1986; Dethier, 2001) or increased amplitude and higher frequency of climatic changes (i.e., glacial-interglacial cycles) during Pleistocene time (Connell et al., 2005; Zhang et al., 2001), particularly after 0.8-0.9 Ma (Morrison, 1991a). In the arid southwest, these oscillations of glacial-interglacial cycles can alter sediment budgets and appear to have played an important role in surficial processes (Hawley et al., 1976; Gile et al., 1981; Morrison, 1991b; Bull, 1990; Imbrie et al., 1993; Winograd et al., 1997). The second potential driver is tectonic uplift (Dethier et al., 1988; England and Molnar, 1990; Pazzaglia and Kelley, 1998; Dethier, 2001; Karlstrom et al., 2008; Aster et al., 2009), including inferred epeirogenic uplift in northern New Mexico-southern Colorado (Karlstrom et al., 2010) or downstream normal faulting (Embudo fault in Koning, 2005; La Bajada fault in Minor et al., 2006). Third, drainage capture can increase downstream incision rates, especially if the added drainage area is large and adds substantially to peak discharge downstream (Dethier, 2001). Such drainage integration has occurred in the Rio Grande in the middle Pleistocene (Wells et al., 1987), probably around 440 ka (Machette et al., 2007).

This paper describes and correlates terraces along the Rio Ojo Caliente, and new tephrochronologic and radiometric data are presented that constrain the ages of two terrace strath levels. Two tephra beds were analyzed in the highest extensive terrace and were found to be from the same source in the adjacent Jemez volcanic field. Illustrative stratigraphic relations are found 6 km north of the town of Ojo Caliente, where the La Madera travertine overlies an extensive, low-level Rio Ojo Caliente terrace (Fig. 2; Newell et al., 2004). We discuss these relations and utilize three new uranium series ages from the travertine to constrain the age of this lower terrace. We then argue that sedimentologic trends in the Rio Ojo Caliente terraces and other terraces in the Española Basin support the "Southwest model" regarding landscape stability and river incision/aggradation, summarize terrace ages along the Rio Ojo Caliente, and discuss inflections in the terrace strath profiles. Lastly, we use terrace ages and their strath heights above the active channel to calculate incision rates for the Rio Ojo Caliente during the past 3.7 Ma.

SETTING

The Rio Ojo Caliente is a tributary to the Rio Chama that drains 1100 km^2 of the Tusas Mountains (Fig. 1; U.S. Geological Survey, 2011). The name "Rio Ojo Caliente" is applied for the portion of the river below the confluence of the Rio Vallecitos and Rio Tusas (Figs. 1 and 2). This confluence is located 35 km upriver from the Rio Chama. The Rio Vallecitos and Rio Tusas are perennial streams that drain the west and east sides, respectively, of Mesa de la Jarita – a southern prong of the Tusas Mountains (Fig. 1). Elevations reach 3000-3250 m at the headwaters of these two rivers. Evidence of glaciation at the headwaters of the Rio Vallecitos has previously been noted (Bingler, 1968), but inspection of topographic maps for glacial geomorphic features suggests that the glaciated area is small (10-15 km^2) and restricted to a small number of north facing slopes and valley bottoms above elevations of 2750 m. In the upper part of the Rio Ojo Caliente, flow is perennial and means of monthly discharges range from 11 ft^3/sec (September) to 312 ft^3/sec (May) (for the years 1933 through 2010; U.S. Geological Survey, 2011). However, its lower extent may be dry part of the year. Its valley bottom is underlain by sand and is 0.4-1.1 km in width. About 10 m of Quaternary

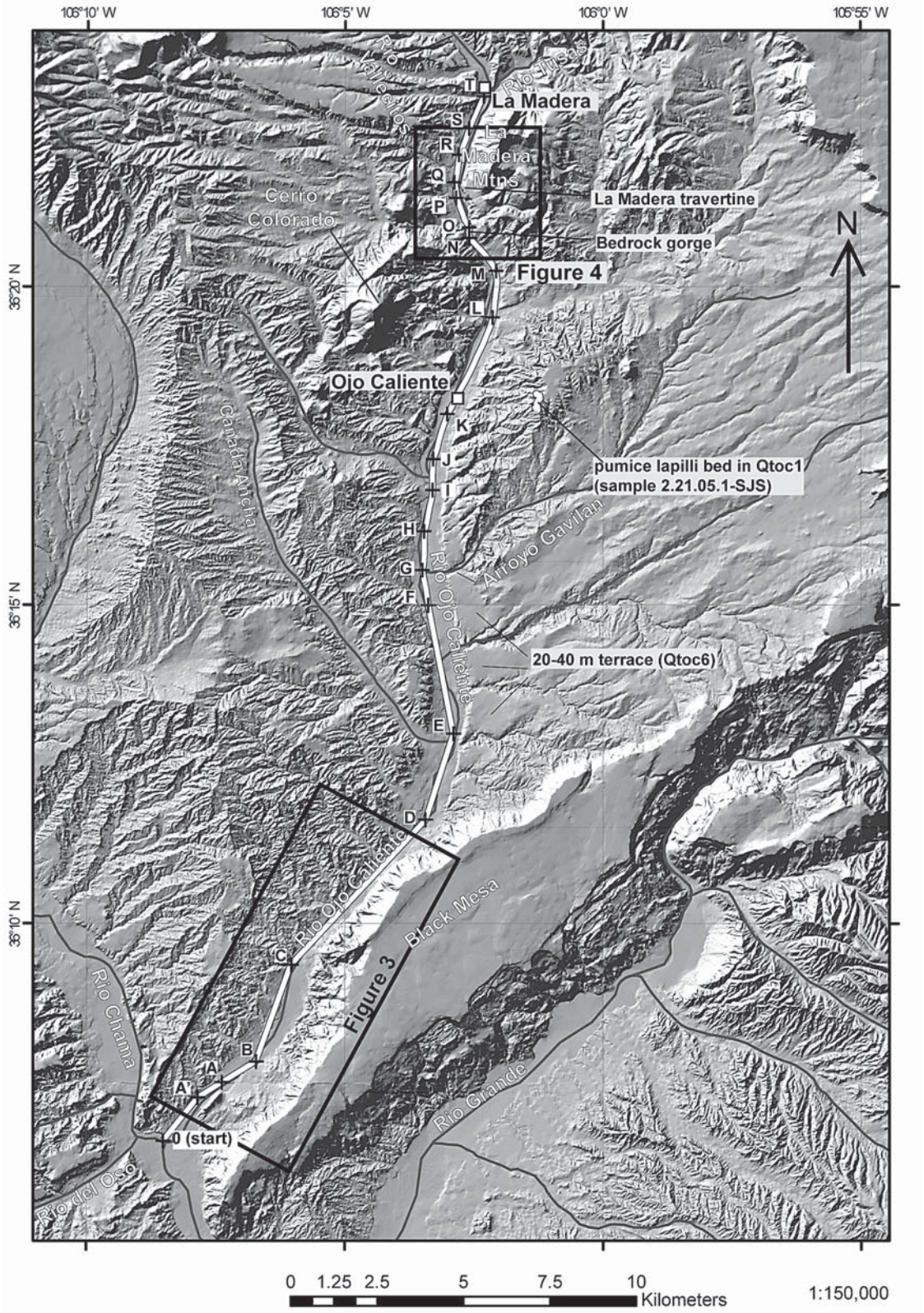

FIGURE 2. Map of Rio Ojo Caliente and study area. Locations of geologic maps of Figures 3-4 are shown by black rectangles. Terrace profile line is shown by the thick, segmented, white line; endpoints of different segments are labeled by letters (Table 4). Dark gray lines depict rivers and streams. Sample location of the pumice-lapilli bed in terrace deposit Qtoc1 is shown (2.21.05.1-SJS).

gravel and clay underlies the valley floor 3 km upstream of the mouth of the river (Wolf, 1996, unpublished consultant report for Ojo de Encantado subdivision along the southern Rio Ojo Caliente). Low discharges tend to be contained in a single channel that exhibits low sinuosity, but a braided pattern develops during high discharges. Because it has surface flow during most of the year, the river supports riparian vegetation and various intensities of human settlement along most of its length. People are concentrated near the town of Ojo Caliente, located 18-26 km above the intersection of the Rio Ojo Caliente with the Rio Chama (Fig. 2).

The Española Basin is a faulted, extensional feature associated with the Rio Grande rift (Kelley, 1978; Manley, 1979) A few nearby faults, such as the Embudo fault system and the southern Ojo Caliente fault, exhibit Quaternary movement (Koning, 2005; Lucas et al., 2005, fig. 1.18). Based on reconstructed terrace strath longitudinal profiles, the Embudo fault has offset a Rio Chama terrace containing the Lava Creek B ash by about 13 m, but offset is difficult to see in profiles of lower terraces (Koning, 2005). The Ojo Caliente fault extends along the west side of the Rio Ojo Caliente, and crosses the river 0.5-1.0 km upstream of the Rio Chama (Koning et al., 2011a, fig. 1). The southernmost part of the Ojo Caliente fault has offset a late Pleistocene Rio Chama terrace by 0.3 m (Lucas et al., 2005, fig. 1.8), but has produced no notable offsets where it extends under various Quaternary terrace deposits along the Rio Ojo Caliente (Fig. 3). Historical subsidence of 2 cm has been noted in repeated leveling surveys near the intersection of the Rio Chama and Rio Ojo Caliente (Reilinger and York, 1979). The cause of this subsidence is not known; it could possibly be tectonic or related to sediment compaction.

Below the confluence of the Rio Vallecitos and Rio Tusas, the Rio Ojo Caliente has incised through moderately to well consolidated, weakly to non-cemented sandstone (with minor conglomerate and mudstone beds) of the Santa Fe Group. North of the town of Ojo Caliente, bedrock highs flank the river (e.g., between the 'N' and 'O' on Fig. 2). At a location 4 km south of La Madera (31 km north of the Rio Chama), the Rio Ojo Caliente has incised a narrow, 0.4 km-long gorge into Precambrian quartzite bedrock (Fig. 2). More narrow, bedrock gorges are found along the lower Rio Vallecitos to the north (see First-Day road log). The Rio Ojo Caliente flows south except for its southern 14 km, where it flows southwest parallel to the general trend of Black Mesa. There are many tributaries entering the Rio Ojo Caliente south of La Madera. All of these tributaries lack surface flow (except during intense summer precipitation events).

DATING METHODS

Two dating methods were used to constrain the ages of two terrace levels. The first is tephrochronology. Three samples of a tephra from the highest correlated terrace were analyzed by electron microprobe at the U.S.G.S. and New Mexico Institute of Mining and Technology. Samples were mounted in epoxy, polished flat, and then examined using backscattered electron imaging (BSE). Selected glass particles were quantitatively analyzed. The details of the electron microprobe analysis are summarized in Table 1 along with sample analytical precision, based on replicate analyses of standard reference materials. Analyses are normalized to 100% to allow for quantitative comparisons between glass compositions in different samples or to compositions of possible source eruptions. However, un-normalized analytical totals are also reported to provide information about the degree of glass shard hydration within individual samples.

The difficulty of distinguishing between compositionally similar eruptive products was recognized several decades ago by tephrochronologists in the western United States, who sought to develop more rigorous statistical methods for tephra correlation (e.g. Sarna-Wojcicki et al., 1987). Methods proposed by Sarna-Wojcicki have been refined to a statistical difference method that has been applied to tephrochronology in volcanic fields with a number of chemically similar eruptive units (Hillenbrand et al., 2008; Kuehn and Foit, 2006; Perkins et al., 1995), provided that precise and accurate geochemical composition, preferably determined on glass, are known for both the source and the tephra layer. The method that we have chosen for data assessment involves calculation of the Euclidean distance function, D (in standard deviation units), between chemical analyses and is only applicable to compositionally homogenous tephra layers (Perkins et al., 1995). The distance function takes into account the analytical error on the analyses, and therefore more heavily weights elements with higher analytical precision. In the case of the analyses presented in this study, the elements that are used in the statistical difference calculations are Fe, Ca, Ti, Mg, Mn and K. The precision on determinations of Si, Al, P, Na and F tends to be lower, either due to analytical constraints, low abundances, or, as in the case of Na, volatility under the beam, particularly at small beam sizes, so these elements are not included. If two analyses were perfectly identical, the D value would be 0. However, because of normal statistical error for techniques used in shard analysis, the mean composition of two, coarse-grained, chemically identical tephra samples, such as those analyzed in this study, will typically have a D value of around 4 (Perkins et al., 1995). Any value below 10 suggests a high degree of similarity between samples.

U-series dating was used to constrain travertines near a prominent terrace 19-30 m above modern river grade. Clean, densely crystalline travertine samples were chosen for U-series analysis to minimize thorium contamination from clays and to lessen the possibility of later calcite precipitation that would produce ages too young for the terraces. Travertine samples were slabbed and micro-drilled to collect ~500 mg of calcite powder for analysis. Powders were dissolved and U and Th were separated by column chemistry. U and Th were loaded on separate filaments and analyzed by thermal ionization mass spectrometry (TIMS) at the University of New Mexico Radiogenic Isotope Laboratory.

TERRACE STRATIGRAPHY

Nomenclature

Seven terraces were mapped and correlated along the Rio Ojo Caliente in the Chili, Lyden, Ojo Caliente, and La Madera 7.5-minute quadrangles. Results of this mapping effort are exhibited in Figs. 3 and 4. Terraces are labeled Qtoc1 through Qtoc7, with

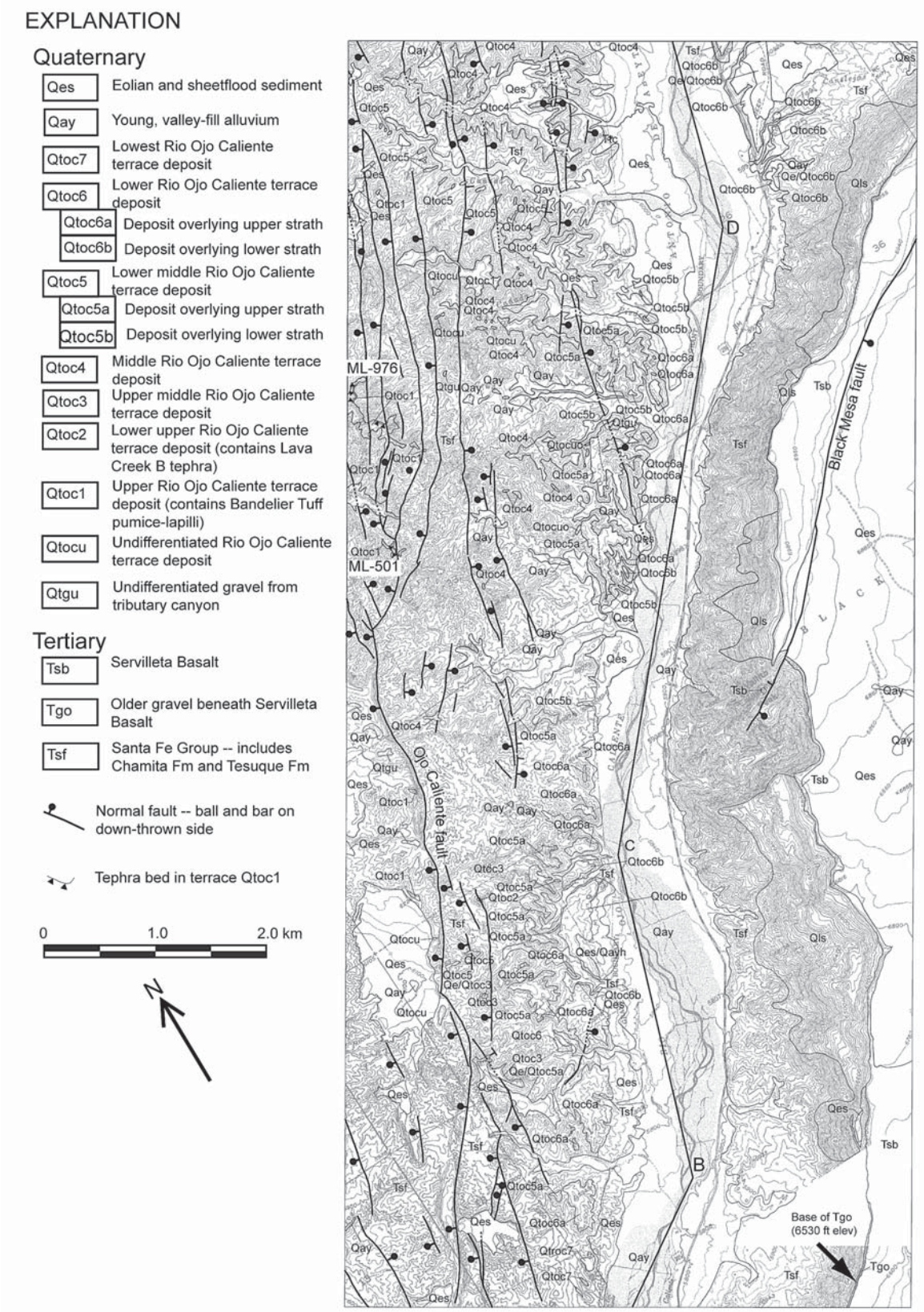

FIGURE 3. Geologic map of the southern Rio Ojo Caliente (see Fig. 2). Terrace profile line is shown, as well as ash sample localities ML-501 and ML-976.

TABLE 1. Average chemical composition (in wt.%) of tephra shards, and representative compositions of suggested correlative eruptions, determined by electron microprobe
Analyses are normalized to 100% oxide total, to correct for variable amounts of fluids in the volcanic glass, mostly water of hydration.

Sample Number	n	P_2O_5	SiO_2	SO_2	TiO_2	Al_2O_3	MgO	CaO	MnO	Fe_2O_3	Na_2O	K_2O	F	Cl	Total (percent)	grain size (microns)¥	Interpreted correlation
Compositions of tephra layers in the study area																	
2-21-05-1-SJS* mean	25 shards	**0.04**	**76.99**	**0.00**	**0.08**	**11.92**	**0.01**	**0.25**	**0.08**	**1.61**	**3.88**	**4.88**	**0.11**	**0.31**	**~100**	500	**Guaje Pumice (D=3.67)**
Mean (original value on analysis)		0.04	73.26	0.00	0.07	11.34	0.01	0.24	0.08	1.38	3.69	4.64	0.10	0.30	95.15		**Tsankawi Pumice (D=4.92)**
Standard Deviation		0.02	0.66	0.00	0.02	0.13	0.03	0.02	0.02	0.08	0.72	0.96	0.07	0.01	0.60		
ML-501-111103-djk mean**	20 shards	**n/a**	**76.60**	**n/a**	**0.12**	**12.31**	**0.04**	**0.30**	**0.06**	**1.44**	**4.53**	**4.61**	**n/a**	**n/a**	**~100**	80 - 150	**Guaje Pumice (D=4.46)**
Mean (original value on analysis)			72.33		0.11	11.63	0.03	0.28	0.05	1.22	4.28	4.35			94.294		**Tsankawi Pumice (D=6.46)**
Standard Deviation			0.63		0.05	0.16	0.02	0.04	0.02	0.09	0.23	0.21			0.90		
ML-976-080504-djk mean**	20 shards	**n/a**	**76.69**	**n/a**	**0.08**	**12.28**	**0.03**	**0.28**	**0.05**	**1.5**	**4.39**	**4.69**	**n/a**	**n/a**	**~100**	80 - 150	**Guaje Pumice (D=3.52)**
Mean (original value on analysis)			71.76		0.08	11.49	0.03	0.26	0.05	1.26	4.11	4.39			93.43		**Tsankawi Pumice (D=4.31)**
Standard Deviation			1.68		0.03	0.25	0.02	0.03	0.03	0.10	0.63	0.27			1.97		
ML-696-310304-djk mean**	18 shards	**n/a**	**76.63**	**n/a**	**0.1**	**12.41**	**0.02**	**0.52**	**0.03**	**1.46**	**3.80**	**5.03**	**n/a**	**n/a**	**~100**	80 - 150	**Lava Creek B (D=2.49)**
Mean (original value on analysis)			72.13		0.10	11.68	0.02	0.49	0.03	1.24	3.58	4.73			93.99		
Standard Deviation			0.46		0.03	0.13	0.01	0.05	0.01	0.15	0.47	0.24			0.82		
Comparative compositions of known widespread tephra layers																	
Lava Creek B ash bed, 0.639 Ma																	
Lava Creek B* grand mean	30 shards	**0.01**	**76.25**	**0.01**	**0.11**	**12.47**	**0.01**	**0.52**	**0.02**	**1.64**	**3.58**	**5.18**	**0.22**	**0.14**	**100.00**		
Standard Deviation		0.02	0.47	0.01	0.04	0.23	0.01	0.04	0.03	0.18	0.13	0.23	0.17	0.03	0.01		
Lava Creek B grand mean**	28 samples	**n/a**	**76.64**	**n/a**	**0.11**	**12.38**	**0.02**	**0.53**	**0.03**	**1.56**	**3.53**	**5.11**	**n/a**	**n/a**	**~100**	**80 - 150**	
Standard Deviation	~500 shards		0.42		0.01	0.17	0.01	0.01	0.01	0.05	0.15	0.19					
Tsankawi Pumice Bed, 1.25 Ma																	
Tsankawi Pumice grand mean**	7 samples	**n/a**	**76.95**	**n/a**	**0.05**	**12.22**	**0.01**	**0.23**	**0.09**	**1.57**	**4.37**	**4.51**	**n/a**	**n/a**	**~100**	**80 - 150**	
Standard Deviation	~125 shards		0.20		0.01	0.09	0.00	0.04	0.01	0.06	0.04	0.11					
Tsankawi Pumice grand mean**	30 shards	**0.01**	**76.77**	**0.02**	**0.06**	**12.14**	**0.01**	**0.28**	**0.06**	**1.64**	**4.10**	**4.51**	**0.20**	**0.32**			
Standard Deviation		0.02	0.59	0.02	0.03	0.16	0.01	0.03	0.05	0.13	0.47	0.20	0.11	0.04			
Guaje Pumice Bed, 1.60 Ma																	
Guaje Pumice* grand mean	30 shards	**0.01**	**76.86**	**0.01**	**0.04**	**12.26**	**0.01**	**0.27**	**0.06**	**1.48**	**4.31**	**4.36**	**0.25**	**0.23**			
Standard Deviation		0.02	0.56	0.02	0.03	0.24	0.01	0.03	0.04	0.10	0.30	0.17	0.10	0.02			
Guaje Pumice grand mean**	7 samples	**n/a**	**77.04**	**n/a**	**0.05**	**12.37**	**0.01**	**0.25**	**0.08**	**1.40**	**4.13**	**4.64**	**n/a**	**n/a**	**~100**	**80 - 150**	
Standard Deviation	~105 shards		0.18		0.01	0.17	0.00	0.01	0.01	0.03	0.24	0.22					

Notes:

* Analysed at New Mexico Tech were performed using a Cameca SX100 electron microprobe with the following analytical conditions: accelerating voltage of 15 kV and probe current of 10 nA. Peak count times of 20 seconds were us
F (100 sec), Cl (40m sec) and S (40 sec). Beam size of 25 micrometers was used in order to avoid Na volatilization. ZAF techniques were used for matrix correction calculations
Background counts were obtained using one half the times used for peak counts. Analyses are normalized to 100 wt.%. N equals number of analyses. Analytical precision, based on replicate
analyses of standard reference materials of similar composition to the unknows, are as follows (all in wt.%): P2O5±0.02, SiO2±0.47, SO2±0.01, TiO2±0.03, Al2O3±0.12, MgO±0.07, caO±0.02, MnO±0.06, FeO±0.06,
Na2O±0.55, K2O±0.27, cl±0.07.

** Analyzed by U.S. Geological Survey Tephrachronologic Laboratory, Menlo Park, Calif. The following analytical conditions were used: 10.05-nA, 15-KV beam current, 10-micrometer beam diameter.
Acquisition time for all elements was 20 seconds, except for sodium , for which a 10 second acquisition time was used to minimize dispersion of sodium ions away from the electron beam.
Standards used are: GSC (Corning Glass Standard), An40 (anorthite), and a homogenous obsidian from La Puebla, Mexico, which was used as an internal standard. The ZAF data-reduction program was used to obtain oxide concentra
Replicate analyses of internal and external standards over the past 25 years indicate that analyses are mutually compatible , despite differences in instrumentation during this time.
Precision and accuracy of the analyses for each oxide are indicated by replicate analysis of RLS-132, and by comparative values from wet-chemical analysis of this standard.
USGS laboratory numbers for samples: 5354 for ML-501, 5355 for ML-696, and 5356 for ML-976.

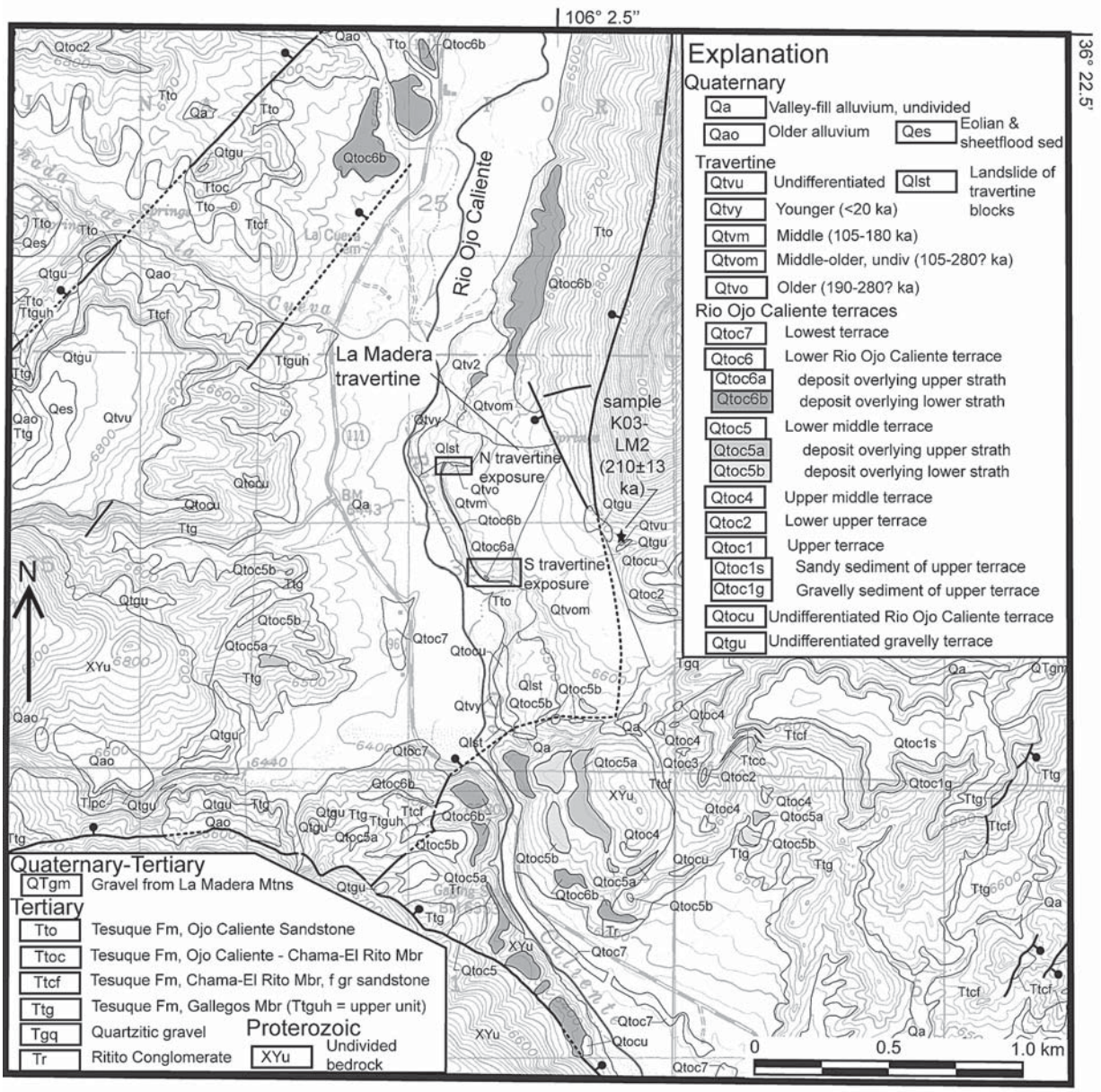

FIGURE 4. Geologic map of the northern Rio Ojo Caliente (see Fig. 2). The La Madera travertines are labeled. The black star depicts the location of a travertine sample that returned a U-series age of 210 ± 13 ka (Table 6). This travertine cements a high-level gravel that may correlate to the Qtoc4 or Qtoc5 terrace. Photographs of La Madera travertine are shown in Figures 10-11 for the two areas outlined by rectangles.

Qtoc1 being the oldest (note that "oc" stands for Ojo Caliente). In a previous paper, we named terraces with lowest as Q1 and highest as Q10 (Newell et al., 2004). The reverse convention is used here to follow work elsewhere in the Española Basin. Table 2 compares and correlates the nomenclature used in Newell et al. (2004) to the one used here. In two of the terraces, Qtoc5 and Qtoc6, two strath levels are noted that are buried by the same terrace fill (Figs. 5-7). The straths of Qtoc5a and Qtoc5b are separated by 7-10 m, and the straths of Qtoc6a and Qtoc6b are separated by 2-7 m. Two terraces are noted on Fig. 5, labeled Qtocu and Qtocy, which are of limited extent and not correlated. Table 3 compares the terrace nomenclature of the Rio Ojo Caliente with that developed on the lower Rio Chama (Koning and Manley, 2003; Koning, 2005).

Profiles of terrace straths and the modern Rio Ojo Caliente

The elevations of the base of terraces (i.e., terrace straths) are plotted as a function of distance upstream from the confluence of the Rio Ojo Caliente with the Rio Chama in Fig. 5 and schematically depicted in Fig. 6. The elevations were projected orthogonally onto straight-line segments that followed the present-day

TABLE 2. Comparison of terrace nomenclature and strath heights between Newell et al. (2004) and this study .

Newell et al. (2004)	This study
Black Mesa	Tgo
Q10 (152-164)	Not correlated along river
Q9 (134-142)	Qtoc1 (107-142)
Q8 (113-128)	Not correlated along river
Q7 (82-122)	Qtoc2 (95-103)
Q6 (67-98)	Qtoc3 (84-88) and Qtoc4 (60-80)
Q5 (67-82)	Not correlated along river
Q4 (55)	Qtocu (56-59)
Q3 (30-61)	Qtoc5 (30-40)
Q2 (14-49)	Qtoc6 (19-30)
Q1 (3-12)	Qtoc7 (5-16)

Note: Numbers in parenthesis are strath heights above modern river (in meters).

river. These segments and their labeled endpoints are illustrated in Fig. 2 and the coordinates of their endpoints are listed in Table 4. Note the irregular nature in elevations of some of the terrace straths. This is interpreted to be due to uneven topography at of the base of the terraces (e.g., Qtoc6b). The apparent irregular nature of the terrace straths is also an artifact of the orthogonal projection. Inspection of geologic maps indicates that the bases of most terraces generally slope orthogonally towards the modern river. For the higher terraces (i.e., Qtoc1 through Qtoc4), strath measurement sites vary in their distance from the river, due to poorer preservation of these terraces. Given the orthogonal slope, the varying distances from the river would create an apparent irregular topography in the terrace strath profiles, particularly for terraces Qtoc1 through Qtoc4.

Two inflection points are present in the profiles, in which the stream profile steepens upstream (Fig. 5). The modern stream and terrace Qtoc6 steepen 21 km above its intersection with the Rio Chama (from 0.3° to 0.4-0.5° average slopes; upstream of H on Fig. 5). Higher terraces (Qtoc1 through Qto5), do not record such an inflection. A second inflection occurs 12-17 km upriver of the Rio Chama (from 0.3° to 0.4° average slopes). All the terrace profiles record this second inflection or are consistent with it. However, the modern stream does not have a notable inflection here. These inflections are further discussed below.

Description of terrace deposits

Here, we present a general description of the terrace deposits (summarized from Koning, 2004, and Koning et al., 2005) and note their thickness variations. The lower part of each of these seven terraces is composed of pebbles, cobbles, and sand deposited by the Rio Ojo Caliente. This basal gravel is generally 2-6 m in thickness and inferred to represent channel and bar deposits. Gravels are clast-supported, rounded, poorly sorted, and include up to 10% boulders. The sand is fine to very coarse, poorly sorted, rounded to subrounded, and rich in lithic grains. Very coarse

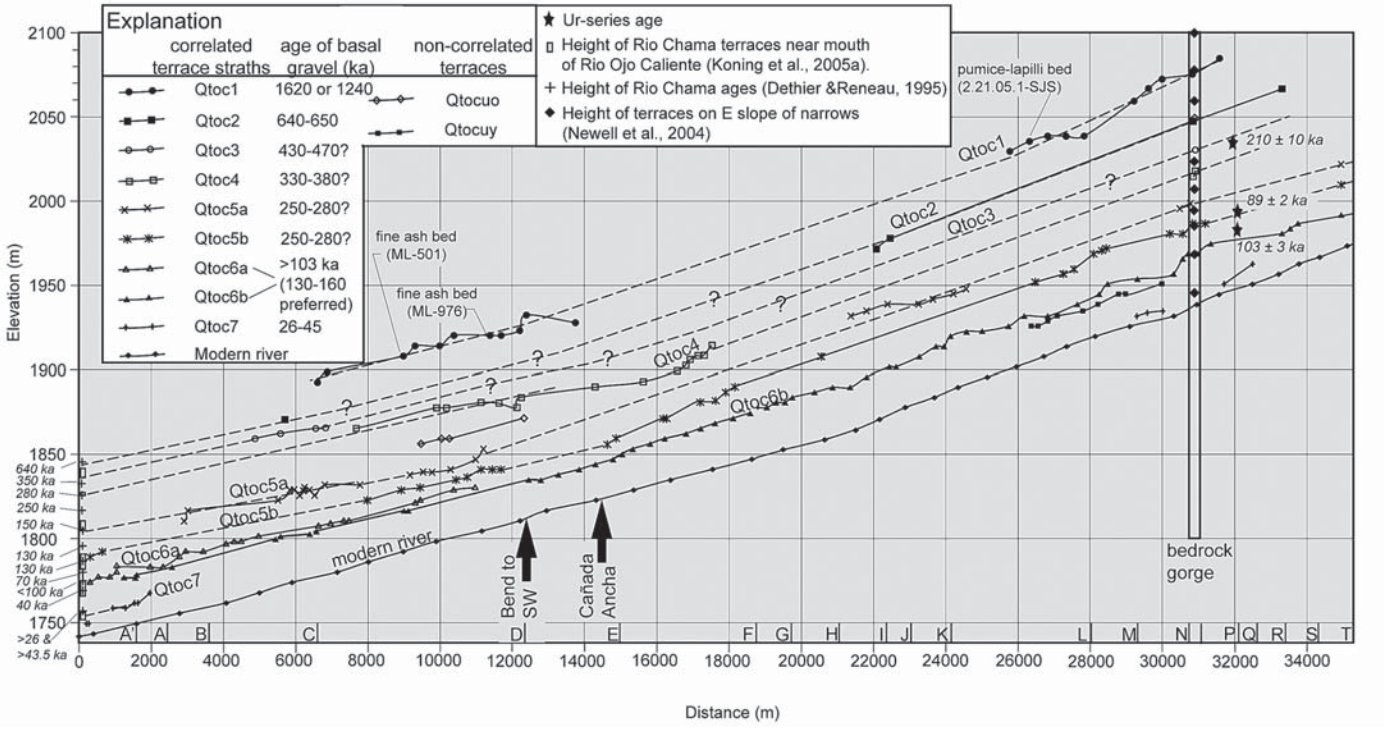

FIGURE 5. Profile of terrace straths along the Rio Ojo Caliente. Distance is measured upstream (to right) from the Rio Chama-Rio Ojo Caliente confluence. Heights of Rio Chama terraces and Rio Chama age control are depicted along the left axis. Location of the segmented profile line is shown in Figure 2. Terrace straths were projected orthogonally onto this profile line.

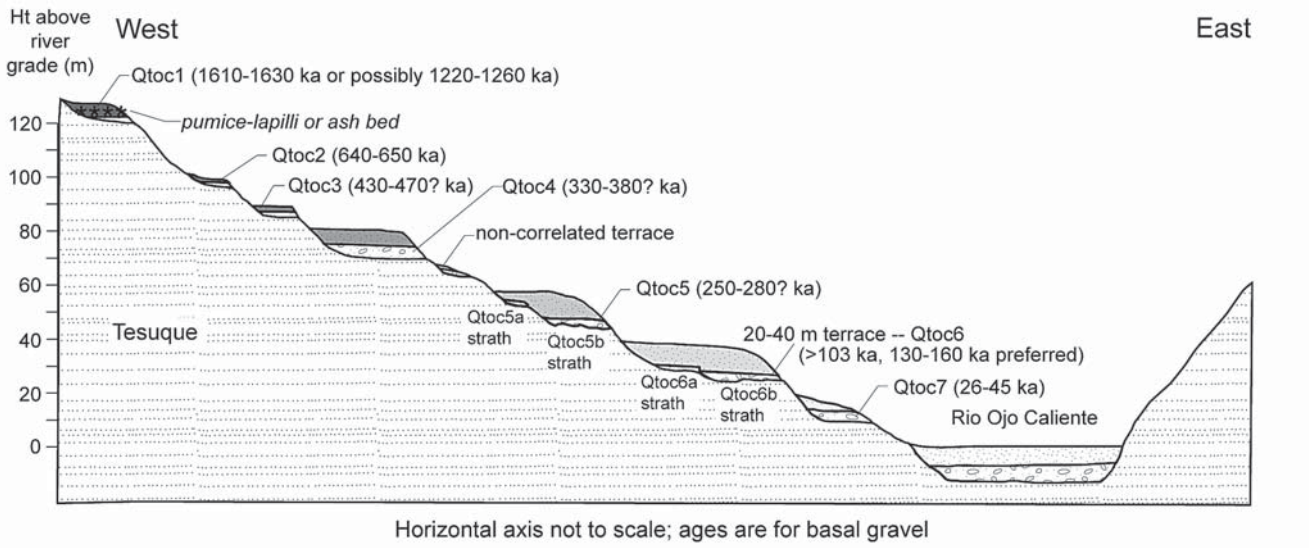

FIGURE 6. Schematic west-east profile illustrating heights, stratigraphy, known ages, and estimated ages (queried) of terraces along the southern Rio Ojo Caliente.

pebbles and cobbles contain subequal amounts of quartzite and volcanic clasts, but very fine to coarse pebbles are typically dominated by felsic to intermediate volcanic clasts. Minor Proterozoic schist, gneiss, granite and metavolcanic rocks are also present in the gravel fraction. Gravel beds are 10 to 50 cm thick and lenticular (internal very thin to thin, planar-horizontal beds are locally present in the medium to thick beds). It should be noted that quartzite and other basement clasts in the terrace gravel are derived from Proterozoic-cored bedrock highs in the Tusas Mountains, composed of the Ortega Quartzite (Hondo Group) or Vadito Group (Williams, 1991; Koning et al., 2007; Aby et al., 2010), or erosion of Eocene-Oligocene conglomeratic units dominated by basement-derived clasts (i.e., El Rito and Ritito Conglomerate of Smith, 1938; Logsdon, 1981; Barker, 1958). The felsic to intermediate volcanic clasts are derived from erosion of the conglomerate and sandstone of the upper Oligocene Los Pinos Formation (Manley, 1981) and Miocene Tesuque Formation (mapped and described in Koning, 2004; Koning et al., 2005b; Koning et al., 2007; Koning et al., 2011b).

The basal, 2-6 m-thick terrace gravel deposited by the Rio Ojo Caliente is generally overlain by <2 m of fine-grained floodplain deposits. The floodplain deposits are overlain by up to 18 m of interbedded gravel and sand (mostly sand). The latter was mostly deposited by local tributary drainages as alluvial fans (similar to those described in Dethier et al., 1990, and Dethier and Reneau, 1995), with subordinate (but variable) contributions by the axial river. This upper sediment largely consists of sand and volcanic pebbles reworked from the Tesuque Formation. Broad surfaces formed on the older, higher terraces have a surficial, sandy unit. This unit is 1-7 m thick and interpreted as a mixture of eolian and sheetflood deposits.

The lowest terrace, Qtoc7, is only preserved in the southernmost Rio Ojo Caliente and adjacent to the bedrock narrows (Fig. 5). Its strath is 5-16 m above the modern stream. Being relatively low, it is buried locally by younger sediment shed from nearby hills or higher terraces. The quartzite-rich, axial gravel is less than 6 m thick.

In contrast to terrace Qtoc7, terrace Qtoc6 is well-preserved and extends the entire length of the Rio Ojo Caliente (Figs. 3-5). This terrace has two straths (Qtoc6a and Qtoc6b) separated by 2-7 m of height (Fig. 5). This terrace is noteworthy in its thickness variations. In its southern 12 km, this terrace has a thick upper part composed of sandy fan or piedmont alluvium up to 18 m-thick that extends across both straths (Fig. 7). In this sandy alluvium are scattered basaltic boulders (1-3% of gravel) whose maximum size is 2.7 x 1.5 m (a and b axes; note that basalt boulders are smaller at site ML-113 in Fig. 8). However, Qtoc6 to the north is only 3-6 m-thick and lacks basalt boulders. The surface of this terrace hosts abundant archeological sites, including pueblo ruins and agricultural plots. Its lower strath (Qtoc6b) lies 19-30 m above the Rio Ojo Caliente. This terrace is also referred to as the 20-40 m terrace, based on the strath height here and elsewhere in the Española Basin (Table 5).

Terrace Qtoc5 is similar to Qtoc6 in that it has two straths generally separated by 7-10 m. These two straths diverge markedly, however, at the southern end of the Rio Ojo Caliente, where they

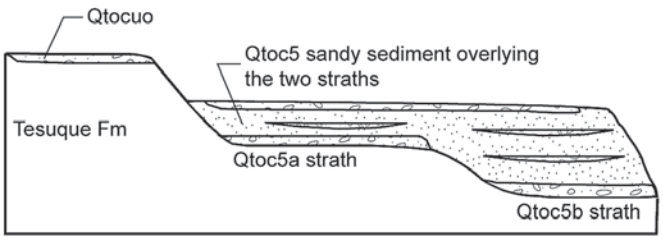

FIGURE 7. Schematic drawing illustrating Qtoc5 stratigraphic relations at site ML-183, located at UTM coordinate 402,440 m E, 4,004,060 m N (NAD27, zone 13).

TABLE 3. Correlation of Rio Ojo Caliente terrace deposits with previous terrace work along the lower Rio Chama

Rio Ojo Caliente terrace unit (this paper)	Strath ht along Rio Ojo Caliente (m)*	Rio Chama terrace unit1	Strath ht along Rio Chama (m)[1*]	Rio Chama terrace unit[2]	Strath ht along Rio Chama (m) [2*]	Rio Chama terrace unit[3]	Strath ht along Rio Chama (m) [3*]	Rio Chama terrace unit[4] (denoted by ht of top of axial river gravel in m)	Rio Grande terrace surface[5]
Qtoc1	107-134 m					Qtc1	235-240		Q1?
Qtoc2	95-103	Qtcg1	90-126	Qtrc1	95-100	Qtc3	103-112	110	Q2
Qtoc3	84-88			Qtrc2	85	Qtc4	81-93	90	
Qtoc4	60-80	Qtcg2a	67-84	Qtrc3	64-69	Qtcu	67-70	74	Q3
Qtocuo	56-59	Qtcg2b	50-64			Qtcu	50-55	64	Q3
Qtoc5**	30-47	Qtcg2c	35-47	Qtrc4	40-49	Qtc5	36-45	54	Q3
Qtoc6***	19-30	Qtcg3	27-38	Qtrc5	24-33	Qtc6	21-27	36	Q4
Qtoc7	5-16	Qtcg4	9-12	Qtrc6	10-14	Qtc7	8-13		

Notes:
1) San Juan Pueblo quadrangle (Koning and Manley, 2003); Minipaper on Rio Chama terraces (Koning, 2005); and First-Day Road Log of this volume.
2) Chili quadrangle, which is where the Rio Ojo Caliente flows into the Rio Chama (Koning et al., 2005). There is one terrace on this quadrangle (Qtrc2, whose strath is t 85 m) which is not shown on the table.
3) Medanales quadrangle, upstream of Rio Chama-Rio Ojo Caliente confluence (Koning et al., 2004). Note that we do not list the Qtc2 terrace.
4) Fig. 3 of Dethier and Reneau (1995).
5) Dethier et al. (1988)
* Straths are measured in meters above the height of the modern river.
** Terrace has two strath couplets separated by 7-10 m. Both terrace straths are overlain by thick, locally derived sediment.
*** Terrace has two strath couplets separated by 2-7 m. Both terrace straths are overlain by thick, locally derived sediment.
Ht = height

are separated by 14 m (Fig. 5). To the south (within 13 km of the Rio Chama), these straths are overlain by a thick fill deposit (7-15 m) dominated by locally derived, sandy fan sediment (Fig. 8). At one site, a gravel bed extends across both straths within this upper sediment (Fig. 7). Based on available exposures, the overlying fill appears to be of the same age, although local cut-and-fills of differing ages are possible in this fill or in the sandy middle-upper alluvium of Qtoc6 (e.g., at the La Madera travertine site, as discussed below). North of 13 km, the deposit is less than 12 m-thick. The lower strath of this terrace (Qtoc5b) lies 30-47 m above the modern river.

Terrace Qtoc4 underlies a prominent geomorphic surface north of river kilometer 10, but to the south preservation is poor (Figs. 3 and 5). The axial river sediment is up to 6 m thick, and is overlain by about 12 m of alluvial fan sediment reworked from the Tesuque Formation to the west. The upper surface commonly is covered by sandy surficial deposits (sheetflood and eolian deposits). This deposit is not preserved north of river kilometer 18, and is correlated northward using only a strath deposit at the bedrock narrows (Fig. 5). The strath of Qtoc4 is located 60-80 m above the modern river, but at river kilometer 15-16 the height of the strath terrace seems to be anomalously low (Fig. 5).

Terrace Qtoc3 is only preserved in the lower Rio Chama, where it lies 84-88 m above river grade and is 1-6 m-thick. We differentiate this terrace because it appears to correlate to relatively extensive terraces along the Rio Chama (Table 3). Near the confluence of the Rio Chama and Rio Grande, this terrace and the strath of the overlying terrace, Qtoc2, appear to be buried, at least in part, by the same deposit of locally derived sand and gravel (Koning and Manley, 2003; Koning et al., 2005a).

TABLE 4. Segment endpoints of terrace profile line along the Rio Ojo Caliente.

Profile segment	Easting (m)	Northing (m)
S end	397,225	3,996,520
A'	398,240	3,997,770
A	398,950	3,998,200
B	399,950	3,998,800
C	401,005	4,001,600
D	404,940	4,005,775
E	405,775	4,008,260
F	405,156	4,011,993
G	404,938	4,012,923
H	405,006	4,014,135
I	405,248	4,015,318
J	405,249	4,016,026
K	405,499	4,016,991
L	407,038	4,020,309
M	407,155	4,021,528
N	406,412	4,022,641
O	406,384	4,022,951
P	406,035	4,023,827
Q	406,000	4,024,310
R	406,127	4,025,021
S	406,426	4,025,847
T	406,800	4,026,708

Note: UTM coordinates (NAD 27 and zone

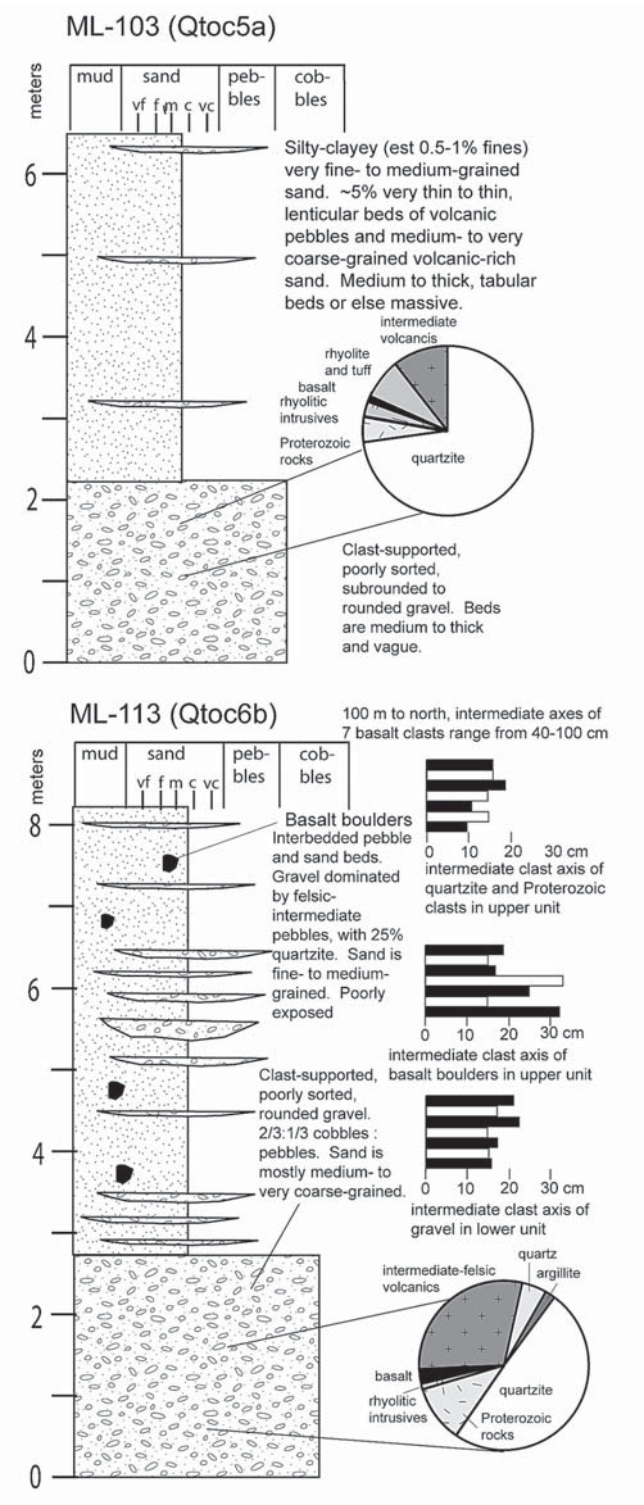

FIGURE 8. Two stratigraphic sections illustrating sediment characteristics of the Qtoc5 and Qtoc6 terraces. Height is measured from terrace strath. Pie graphs show results of clast counts of basal gravel. Bar graphs in ML-113 illustrate range of clast sizes. ML-103 and ML-113 are located at the following respective UTM coordinates (NAD27, zone 13): 399,605 m E and 4,000,710 m N; 400,230 m E, 4,000,850 m N.

Terrace Qtoc2 is an important terrace because it correlates with a Rio Chama terrace that contains Lava Creek B ash beds (Table 3; Dethier et al., 1990). This terrace is poorly preserved along the Rio Ojo Caliente, except at La Madera (Koning et al., 2007). Near La Madera, this terrace underlies a broad (50 km^2) surface and is 5-30 m-thick. This terrace deposit is less than 6 m thick to the south. Its strath lies 95-103 m above the Rio Ojo Caliente (Newell et al., 2004).

The Qtoc1 terrace is found in dissected terrain between river kilometers 6 and 14 km. It forms broad surfaces 26-31 km upstream of the Rio Chama. Qtoc1 is commonly 6-18 m thick, with the upper part composed mostly of sand that is locally derived and possibly mixed with eolian sediment. Its strath is located 107-134 m above the modern river.

On the northwest edge of Black Mesa, there is 1-5 m of ancestral Rio Grande gravel and floodplain deposits underlying Servilleta Basalt (unit Tgo in Fig. 3). This sedimentary package is described in Koning et al. (2011a) and its proximity to our study area is utilized to provide long-term rates of incision for the lower Rio Ojo Caliente. The capping basalt here is 3.6-3.8 Ma based on two $^{40}Ar/^{39}Ar$ ages (3.69±0.25 Ma, Maldonado and Miggins, 2007; 3.65 ± 0.09 Ma, Reneau and Dethier, 1996), so these gravel and floodplain deposits are slightly older (3.7-4.0 Ma). They are not numbered in our terrace nomenclature because they were not deposited by the Rio Ojo Caliente and are Pliocene in age.

Age Control

Qtoc1 and tephra correlation

Terrace Qtoc1 is important for age control because it contains a widely exposed tephra bed. In southern exposures (Fig. 3), this tephra is in a single medium to thick, tabular bed continuous for 10s of meters; very thin to laminated, internal bedding may be present. The bed is composed of a slightly ashy very fine to medium sand, with local 5-10 cm lenses of relatively pure ash – two of which were sampled. This bed is located 3-6 m above the strath of the deposit in sandy, locally derived alluvium. The northern exposures of this tephra are found 2.1 km east of the town of Ojo Caliente (Fig. 2; Koning et al., 2005). Here, the tephra is a pale yellow, pumiceous fine lapilli and coarse ash that occurs in a single, thick bed 4-8 m above the strath. The pumice is 0.1-4 mm in diameter and mixed with crystals of quartz (~5%) and mafics (0.5-1% hornblende or pyroxene and also biotite).

Three samples of this tephra were obtained (Figs. 2-3) and analyzed by electron microprobe (see Methods section). The results of these analyses indicate a strong correlation of these samples with the Bandelier Tuff (Table 1). Correlation to either the Guaje Pumice Bed (Otowi Member) and Tsankawi Pumice Bed (Tshirege Member) is permissible but the samples are slightly more similar to the Guaje Pumice Bed, based on lower D values in Table 5 and CaO vs. Fe_2O_3 comparisons (Fig. 9). The Otowi Member has been dated using $^{40}Ar/^{39}Ar$ methods at 1.61-1.63 Ma (Izett and Obradovich, 1994; Spell et al., 1996a,b) and the Tsankawi Pumice Bed has been dated at 1.22-1.26 Ma (Izett and Obradovich, 1994; Spell et al., 1996a, b; Phillips et

TABLE 5. Correlation of 20-40 m terrace (Qtoc6) across the Española Basin.

River and terrace label	Height of strath (m)*	Total sediment thickness (m)	Quadrangle	Reference	Comments
Rio Ojo Caliente (Qtoc6)	19-30	up to 18	Lyden and Ojo Caliente	This work	Strath couplet vertically separated by 2-7 m. Both straths are buried by same locally derived sediment.
Rio Tesuque (Qgt3)	20-40	up to 18	Horcado Ranch	Koning and Maldonado, 2001	The thick fill diverges upstream into two thinner (1-6 m) and more gravelly terrace deposits. El Cajete pumice fills a gully-fill inset below terrace surface and provides a minimum age constraint.
Junction of Rio Tesuque & Pojoaque River (Qtpt1)	18-35	7-30	Española	Koning (2002)	Base of unit is generally scoured and has up to 25 m of relief.
Pojoaque River (Qtp2)	at least 30	18-25	Cundiyo	Koning et al. (2002)	
Santa Cruz River (Qtsc4)	27-34	10-25	Española	Koning (2002)	
Santa Cruz River (Qtsc2)	27-34	9-18	Cundiyo	Koning et al. (2002)	
Santa Cruz River (Qtsc4)	27-37	up to 18	Chimayo	Koning (2003)	
Santa Cruz River (Qtsc4)	27-34	1-15	San Juan Pueblo	Koning and Manley (2003)	
Junction of Rio Grande & Rio Chama (Qtcg3)	27-38	7-20	San Juan Pueblo	Koning and Manley (2003)	
Rio Chama (Qtrc5)	24-33	Up to 34	Chili	Koning et al. (2005a)	Note thickness of fill.
Rio Chama (Qtc6)	21-27	4-12	Medanales	Koning et al. (2004)	

Note:
* Height of strath above modern river grade.

al., 2007). The fine-grained texture of the southern two samples made the hand sample look similar to ash found in higher terraces along the Rio Chama (Qtc3 of Koning et al., 2004); this ash was correlated to the Lava Creek B Ash (Dethier et al., 1990; sample ML-696 in Table 1). However, the composition of the Lava Creek B ash and the tephra from Qtoc1 clearly differ (Fig. 9).

20-40 m terrace (Qtoc6) and La Madera travertines

The terrace level associated with Qtoc6 has been correlated across the Española Basin based on its strath height (generally 20-40 m), presence of a high-relief strath, and terrace sediment that is 5-34 m-thick, the middle to upper parts of which are locally derived (Table 5). However, the age of the 20-40 m terrace has been somewhat enigmatic. It had previously been assigned a 70-90 ka age based on comparison of its strath height with data in Dethier and Reneau (1995, table 1). The 70-90 ka terrace age was listed in a variety of geologic maps and reports made by the lead author (Table 5). Age constraints for this terrace level were obtained from amino acid racemization ratios of snail shells in the deposit (Dethier and McCoy, 1993) and the fact that the El Cajete tephra is found interbedded in a gully-fill inset into the surface of this terrace level, which provides a minimum age constraint (Table 5; Koning and Maldonado, 2001). The age of the El Cajete tephra has been controversial over the last two decades, but recent studies suggest that it is ~55-60 ka (Toyodo and Goff, 1996; Reneau et al., 1996b). Using a plethora of surface dating techniques (including soil carbonate accumulation, varnish-cation ratios, amino-acid racemization ratios, and uranium-series

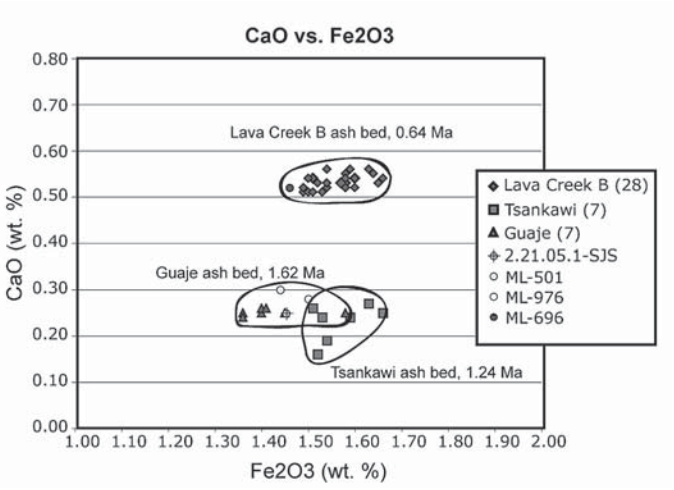

FIGURE 9. Plot of CaO vs. Fe_2O_3 for tephra samples in terraces along the Rio Ojo Caliente and Rio Chama. Data from Table 1.

(U-series) dating of carbonate rinds on clasts), the age of the surface on this terrace was inferred to be 75-135 ka (Dethier et al., 1988).

Our study adds critical age control to this extensive terrace level. This age control comes from U-series dating and stratigraphic relations at the La Madera travertine deposit, which is up to 30 m-thick and located 2.8 km south of La Madera and 6.3 km north of Ojo Caliente (Figs. 2, 4, and 10a). Illustrative exposures are found on the north and south face of the main travertine platform (Figs. 4 and 10a). On the north face, one can see complex stratigraphy typical of travertine mounds. Two areas of steeply inclined drape bedding are present (Fig. 11). Drape bedding is formed when spring waters on a travertine platform spill over a pre-existing cliff face, a modern example which can be observed at the north end of the La Madera travertine (Fig. 10b). A set of 10 m-tall drape beds on the right side of the exposure is thus used to define a small paleo-cliff, and the travertine to the left of the paleo-cliff is older than the travertine to the right of the paleo-cliff (Fig. 11). After the older travertine unit formed, spring waters flowed over its top surface and spilled over the paleo-cliff face on its west (right) side. This water deposited younger travertine on top of the older travertine unit (defined by subhorizontal beds), steeply inclined, ~10 m-tall drape beds on the paleo-cliff face (the right set of drape beds), and relatively massive travertine to the right of the paleo-cliff face (Fig. 11). A left set of drape beds is also observed and it is likely part of the older unit – although there is some ambiguity if all of the drape beds there belong to the older unit, particularly those by the east cave (Fig. 11). The 20-40 m Rio Ojo Caliente terrace (Qtoc6) underlies the westernmost extent of the travertine just to the west of the right set of drape beds, and sparse river gravel, characterized by rounded quartzite clasts, can be found under the travertine at a point about half-way between the present-day edge of the cliff and the right drape-set (Fig. 11). Unfortunately, talus and landslides bury the base of the travertine cliff to the east of the drape.

Flowstone samples were taken from two caves in the northern face of the main platform (Fig. 11; samples K03-LM-4 and -5; Table 6). These caves were formed in the aforementioned two sets of drape beds. These caves clearly cross cut and are developed within the drapes (Figs. 10c, 11). Thus, these U-series ages should be considered as minimum ages for the drapes. The U-series age from the cave that cross cuts the left set of drape beds returned 89 ± 2 ka and the U- series age from the cave crosscutting the right set of drape beds returned 103 ± 3 ka (Table 6). Dates of the non-cave travertine are needed (and underway), but our present interpretation is that the cave pockets develop within the active drapes, similar to the modern caves shown in the active drape of Figure 10b, and thus probably only post-date the drapes by a small amount of time. Hence, the 103 to 89 ka age progression is inferred to be the time of accumulation of the platforms and drapes of much of the main La Madera travertine mound. The 20-40 m (Qtoc6) terrace gravel under the younger unit must be older than 103 ka, so the previous age estimate of 70-90 ka for this terrace is too young. The travertine that overlies the Qtoc6 terrace gravels is likely no more than a few tens of thousands of year older than 103 ka.

Another travertine sample was collected from a high-level, tributary terrace gravel that appears to correlate best to the main stem Rio Ojo Caliente terraces Qtoc4 or Qtoc5 (Fig. 4). Here, a travertine spar vein crosscuts and cements the upper preserved gravel of the sloping terrace. U-series analysis of the cementing travertine returned an age of 210±13 ka (Table 6). This travertine likely pre-dates the Qtoc6 terrace because it cements a higher terrace level (probably before the incision that resulted in the lower Qtoc6 terrace).

DISCUSSION

Fluvial response to climate change

We argue that the "Southwest model," articulated by Hawley et al. (1976), is applicable to the Rio Ojo Caliente in addition to other rivers in the Española Basin. Along the Rio Ojo Caliente and elsewhere in the Española Basin, there are commonly two stratigraphic intervals in a given terrace deposit, as exemplified in Figure 8: 1) a lower level consisting of 1-6 m of clast-supported gravel and 2) an upper level that is sandier than the lower level and generally thicker (where preserved). Included at the base of the upper level is <2 m of floodplain sediment. The lower stratigraphic interval is dominated by gravelly sediment transported long distances by the axial river. Although this basal gravel is difficult to date, we believe it is reasonable to correlate it with higher river discharges from melting snow and possible glaciers during glacial climates. In correlative terraces along the

TABLE 6. Uranium series ages for La Madera travertine.

Sample	^{234}U (ng/g)	^{232}Th (pg/g)	δ^{234}U ‰	^{230}Th/^{238}U activity	Age (yrs)	Comments
K03-LM2	23.6 ± 0.02	1693 ± 35.0	381.4 ± 9.7	1.2607 ± 0.0273	210499 ± 12969	Travertine caps tributary terrace gravel correlative to Qtoc4 or Qtoc5.
K03-LM4	14.8 ± 0.02	5068 ± 61	793 ± 14.8	1.0222 ± 0.0187	103163 ± 3117	Cave flowstone in younger travertine unit directly overlying the Qtoc6 terrace (Figure 11). Provides minimum age for Qtoc6 terrace.
K03-LM5	8.14 ± 0.02	145 ± 17	640.9 ± 9.2	0.9584 ± 0.0152	89237± 2197	Cave flowstone in older travertine unit (Figure 11); no direct stratigraphic relation with terraces.

δ^{234}U measured = (δ^{234}U measured/ δ^{234}U eq -1) x 1000, where δ^{234}U eq is the secular equilibrium atomic ratio (λ238/λ234 = 5.48862 x10-5). Errors are 2-sigma.

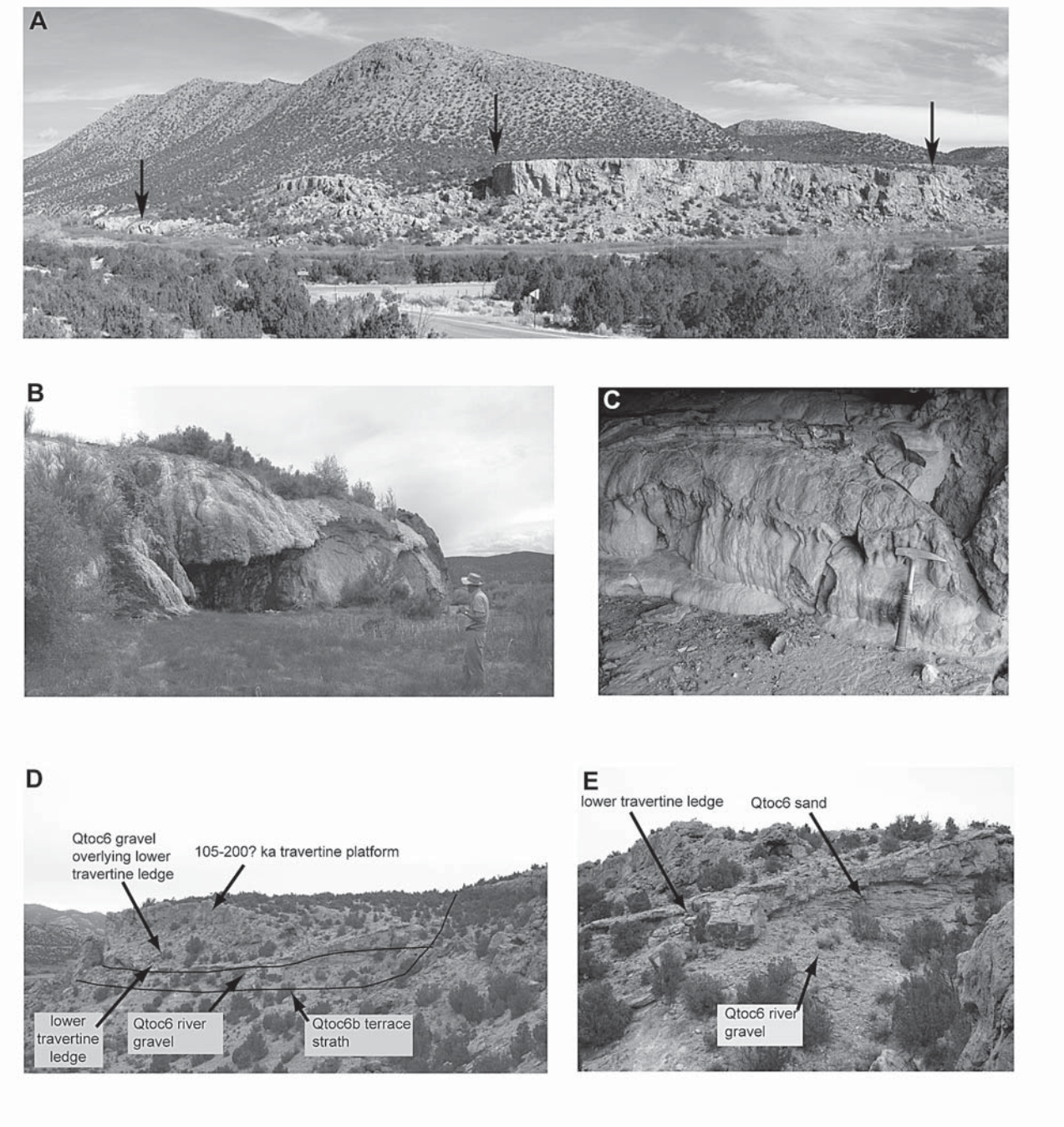

FIGURE 10. Select photographs of La Madera travertines. A): View of the main platform of the travertine complex, looking east (photograph courtesy of Kirt Kempter of GeoMosaics). The La Madera Mountains are in the background. The left arrow points to location of modern travertine precipitation (photograph B), the middle arrow points to the northern exposure of the main platform, and the right arrow denotes the southern exposure of the main platform (photographs D-E); between the middle and right arrows, the near-cliff face overlies quartzite-rich gravel of the 20-40 m terrace (Qtoc6). B) Modern travertine precipitation occurring as steeply inclined drapes. C) Sampled flowstone within a cave that yielded a U-series age of 103 ± 3 ka (see Figure 11). D) View north of the southern exposure of the main travertine platform, Qtoc6 terrace, and buttress unconformity. Note that Qtoc6 gravel is found both below and above the lower travertine ledge, which indicates that the stream experienced another episode of aggradation after precipitation of the lower travertine ledge. The older travertine on the right = Qtvm of Fig. 4. E) Close-up view of the center of the photograph in D. Note the very thin to thin, tabular beds of sand and siltstone overlying the terrace gravel. This sand is very fine- to very coarse-grained, subangular to angular, and moderately to poorly sorted. It was probably locally derived from the La Madera Mountains.

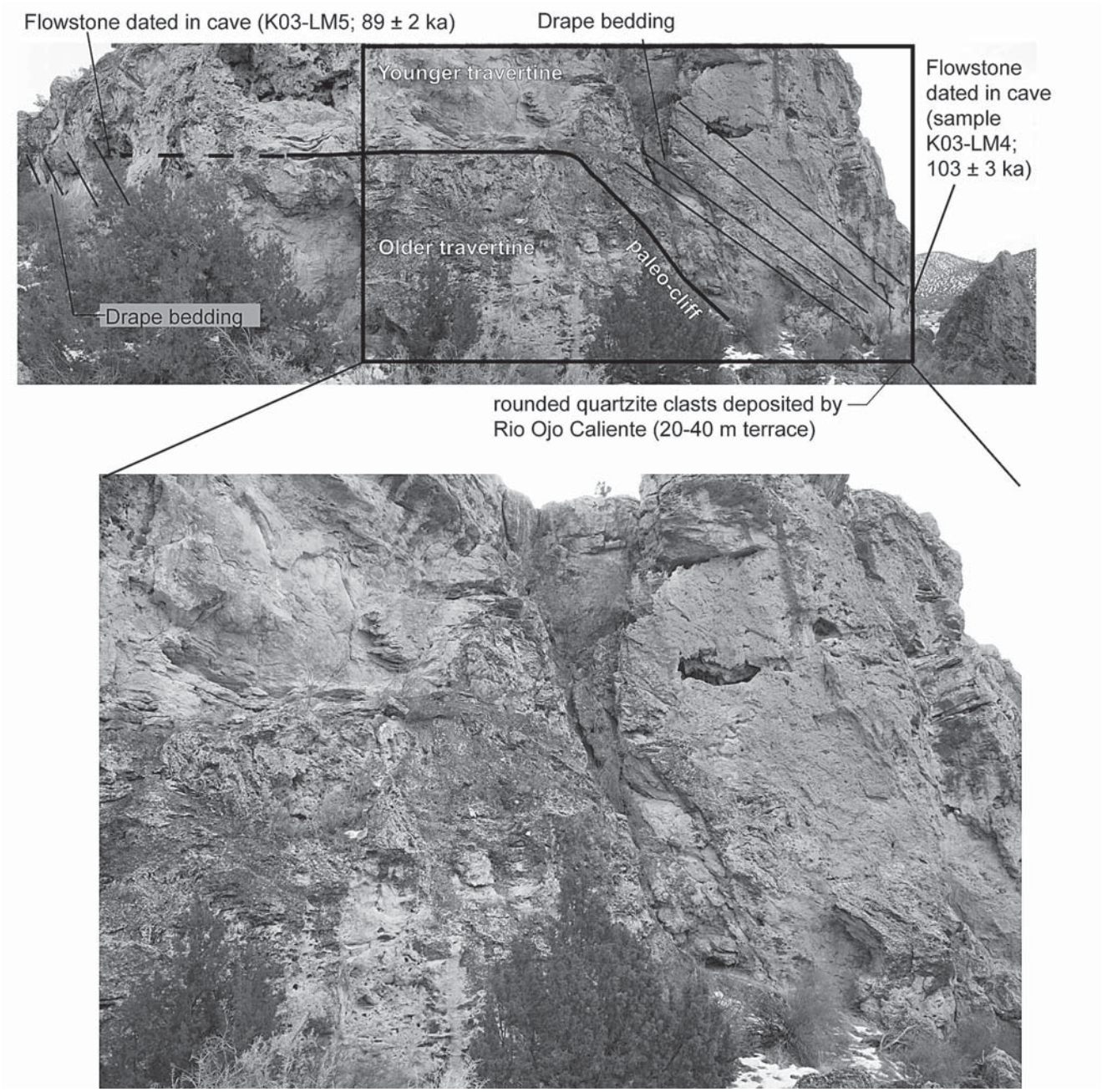

FIGURE 11. Photograph of the northern travertine exposure, view is to the south. An inferred paleo-surface (heavy black line) separates a younger and older travertine unit (these units are labeled Qtvm and Qtvo on Figure 4). Two sets of drape bedding are shown (inclined black lines) and the locations of the 89 ka and 103 ka cave flowstone samples are depicted.

Animas River, for example, the Lava Creek B ash overlies glaciofluvial terrace deposits (Gillam et al., 1984; Gillam, 1998). In the upper stratigraphic interval, the prevalence of locally derived alluvium indicates that sediment contribution by local, low order drainages – probably deposited as alluvial fans on the margins of the valley bottom -- dominated over sediment contribution by the axial river. Within the Española Basin, streams and small rivers sourced in the surrounding highlands experienced sand-dominated sedimentation during the present interglacial (i.e., the Holocene). Studies documenting Holocene sand-dominated, locally derived sedimentation have been done on the lower Rio del Oso immediately south of the mouth of the Rio Ojo Caliente (Hall and Periman, 2007), the Rio Tesuque (Miller and Wendorf, 1958), and on the east margin of the Rio Grande near Española (Johnpeer et al., 1985; Love et al., 1987; Hawley, 1995). Considering the significant component of locally derived sediment in

Holocene deposits of the Española Basin, we suggest that similar sediment observed in the upper part of the Rio Ojo Caliente terraces was deposited during an interglacial climate or possibly during a transition between glacial to interglacial climates – consistent with interpretations by Dethier et al. (1990), Dethier and Reneau (1995), and the "Southwest model" of landscape stability.

The south exposure of the main platform at the La Madera travertine illustrates the dynamic nature of aggradation and erosion along the Rio Ojo Caliente during 105-130? ka. After deposition of the basal gravel overlying the Qtoc6b strath, a thick interval of locally derived sand was deposited, 6-8 m of which is preserved (Fig. 10 e). Following this sandy deposition, stream incision created a relatively steep, westward sloping surface on this sand. Local CO_2-rich springs laden with dissolved carbonate deposited travertine on this slope (the lower travertine ledge of Figs. 10d, e). Subsequent river aggradation resulted in the deposition of quartzite-rich river gravel on top of the lower travertine ledge (Fig. 10d).

The abundance of basalt boulders in the upper part of the 20-40 m terrace (Qtoc6) is noteworthy (Fig. 8). These boulders are only found downstream of segment endpoint C, and must have been derived from the steep slopes of Black Mesa. Higher level terrace deposits do not contain as many basalt boulders. These basalt boulders support the inference of significant local erosion during deposition of the upper, sandy part of the 20-40 m terrace, which we infer occurred during oxygen isotope stage 5. The northwestern slopes of Black Mesa must have been relatively unstable during this time, with boulders transported off the slope via mass wasting. Lateral migration of the river across the floodplain may locally have undercut the northwestern slope of Black Mesa, facilitating mass wasting.

Terrace ages

The ages of three terraces are relatively well constrained along the Rio Ojo Caliente. The highest extensive terrace, Qtoc1, has tephra which correlates to the Bandelier Tuff (Table 1). Correlation is slightly better with the Guaje Pumice Bed of the Otowi Member, but correlation with the Tsankawi Pumice Bed of the Tshirege Member is also permissible (Table 1 and Fig. 9). Pumice-lapilli of this tephra occurs in the lower gravel of the Qtoc1 deposit, whereas the fine-grained ash is found in the sandy, upper part of the Qtoc1 deposit. We infer that the ash represents fluvial reworking of the tephra. Since the pumice-lapilli occurs in the lower gravel, the age of the base of the deposit is close to the age of the pumice bed: 1.61-163 Ma (our preferred age; Izett and Obradovich, 1994; Spell, 1996a,b). An interesting observation regarding Qtoc1 is its lower height (107-134 m) above the modern Rio Ojo Caliente compared to the height of a terrace containing Guaje pumice-lapilli along the lower Rio Chama (235-240 m; Qtc1 of Table 3). Qtoc2, with strath heights of 95-103 m, does not expose any tephra along the Rio Ojo Caliente but it is also poorly preserved here. However, near La Madera this terrace is well preserved and 5-30 m-thick. We correlate Qtoc2 to an extensive terrace along the Rio Chama, whose strath lies 90-126 m above the modern river (Table 3 and Fig. 5). The deposit of this Rio Chama terrace contains several exposures of the Lava Creek B ash in floodplain sediment immediately above the basal terrace gravel (sample ML-696 of Table 5; Dethier et al., 1990). The Lava Creek B ash has recently been dated at 639 ka (Lanphere et al., 2002). Thus, the base of the Qtoc2 terrace is interpreted to be 650-640 ka. The lowest terrace with age control is the 20-40 m terrace. Based on U-series data and stratigraphic relations with the La Madera travertine (elaborated above), the age of the 20-40 m Rio Ojo Caliente terrace (Qtoc6) strath is older than 103 ka and probably younger than 210 ka; our preferred age is 130-160 ka for the terrace strath and basal gravel.

The other terraces (Qtoc3, Qtoc4, Qtoc5, and Qtoc7) are not directly dated along the Rio Ojo Caliente. Terrace levels at similar heights to Qtoc7 along the Rio Grande have yielded radiocarbon ages consistent with a 26-46 ka age (Fig. 4; Dethier and Reneau, 1995; table 1). We can constrain the ages of the remaining terraces (Qtoc3 through Qtoc5) to between 160 and 640 ka based on the ages of Qtoc6 and Qtoc2. A travertine cementing a high-level tributary gravel that may possibly correlate with Qtoc4 or Qtoc5 returned a U-series age of 210 ± 13 ka (K03-LM2 on Fig. 4), which provides a minimum age for this terrace deposit. Near the town of Chama, a possible correlative terrace to Qtoc5, located 49 m above modern river grade, is capped by a basalt flow with a K/Ar age of 240±60 Ma (Scott and Marvin, 1985).

Regardless of whether strath formation occurs during glacial maximums (Hawley et al., 1976; Dethier and Reneau, 1995; Rogers and Smartt, 1996), interglacials (Pazzaglia, 2005), or during the glacial to interglacial transition, it is not unreasonable to associate individual terrace formation with the time encompassing a late glacial to an early interglacial (Fig. 12), although terraces recording such climatic events may not all be preserved.

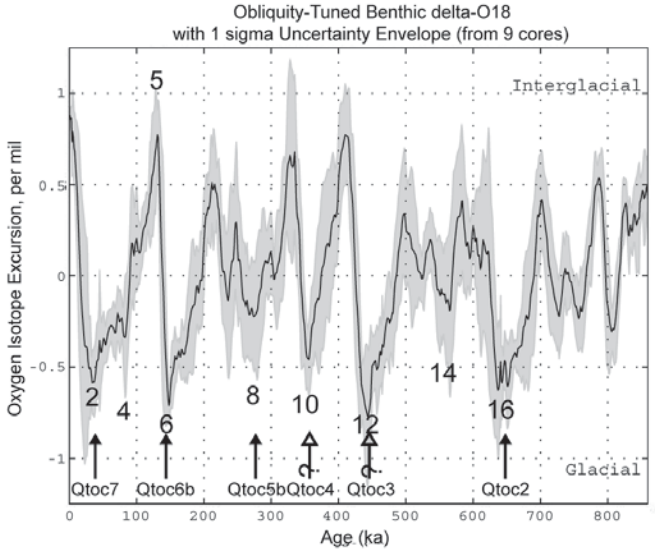

FIGURE 12. Global climate oscillations between glacial and interglacial periods over the last 800 k.y. based on marine oxygen isotopes. Glacial oxygen isotope stages are labeled (2 through 16) as well as our interpreted ages of the basal gravels of various Rio Ojo Caliente terraces. Open arrows denote uncertain ages. Slightly modified from Karner et al. (2002, fig. 8).

Using this approach, and our age interpretation of terrace Qtoc6, we estimate a 280-250 ka age for the base of Qtoc5. This age inference is consistent with the 280 and 250 ka ages inferred from amino-acid racemization ratios (Dethier and Reneau, 1995; table 2; Fig. 5), the U-series age of 210 ± 13 ka at the top of the terrace (Fig. 4; sample K03-LM2 of Table 6), and the aforementioned 240 ka basalt capping the 49 m-high terrace near Chama. The base of Qtoc4 may be associated with oxygen isotope 10 (380-340 ka) or the oxygen isotope 10-9 transition (340-330 ka). This age inference is consistent with the 350 ka age inferred from amino-acid racemization ratios (Dethier and Reneau, 1995; table 2; Fig. 5). Terrace Qtoc3 may possibly have been deposited during oxygen isotope stage 12 (430-470 ka) or shortly afterwards. No amino acid ratio data are available to compare with this terrace level and its age is highly uncertain.

Inflections in terrace strath profiles and the modern river

As noted earlier, there appear to be two inflections in the Rio Chama terrace straths. First, the modern river and the lower Ojo Caliente terrace exhibit inflections in their profiles at a location 21 km above the intersection of the Rio Ojo Caliente and the Rio Chama. This inflection location coincides with a rock type change in the Tesuque Formation of the Santa Fe Group at the mouth of Arroyo Gavilan (Fig. 2; Koning et al., 2005b). South of here, strata are mostly sandstones of the Chama-El Rito Member and Ojo Caliente Sandstone Member. North of here, strata generally belong to the Duranes Member (Koning et al., 2011b), which is dominated by sandy conglomerate and pebbly sandstone. The contact between the gravelly Duranes Member and overlying sandy strata strikes NNE and dips 3-6° ESE, and projects underneath the Qtoc6 terrace at an elevation of 1820 m (Koning et al., 2005b). It is difficult to evaluate how this lithologic change influenced the profiles of higher terraces because of the discontinuity of these higher straths (i.e., these straths are not preserved in the proximity, and on either side, of the dipping contact, as shown in Koning et al., 2005b).

An inflection of the Qtoc4 and Qtoc5 terrace straths occurs 12-17 km upriver of the Rio Chama. This inflection is located close to the mouth of Cañada Ancha (Fig. 2). In this area, the Rio Ojo Caliente begins to bend southwestward and parallel to the trend of Black Mesa. There is no notable rock type change in the Tesuque Formation in this area and the profile inflections are difficult to explain.

Incision rates

We update and extend the Newell et al. (2004) incision rate curve to the lower Rio Ojo Caliente using terrace elevations measured between river kilometers 2 and 7 (Fig. 13). Incision rates are calculated between terraces with age control (i.e., gravel near top of Black Mesa, terraces Qtoc1 and Qtoc2, terrace Qtoc6, and the modern river). Compared to the earlier calculations of Newell et al. (2004), general trends in incision rates have not changed. There was a moderate average rate of incision of 51-60 m/Ma between 3.7 Ma and 1.2-1.6 Ma (age of Qtoc1). A low average

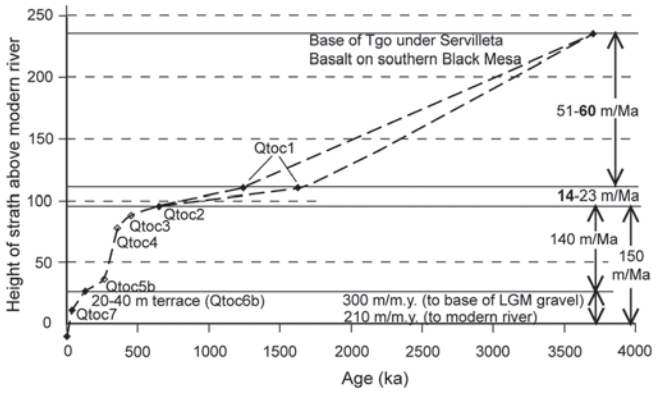

FIGURE 13. Graphical representation of incision rates along the Rio Ojo Caliente for the past 3.7 Ma. Note that aggradation episodes are not depicted. Heights of terrace straths were measured in the vicinity of profile segment endpoint C except for Qtoc7 and the base of the gravel underlying Servilleta Basalt on Black Mesa (Tgo), which were measured in the vicinity of segment endpoints A and B, respectively. Note that the Qtoc5a and Qtoc6a straths are not shown. For calculating terrace rates, the median of the age range for a given terrace base was used (see Figure 5 for summary of age ranges); age of the Tgo gravel is from the age of the overlying basalt (3.69±0.25 Ma; Maldonado and Miggins, 2007; 3.65 ± 0.09 Ma, Reneau and Dethier, 1996). The ranges of incision rates for the time between gravel Tgo and Qtoc1, and between Qtoc1 and Qtoc2, is due to the two possible ages of Qtoc1 (depending whether the tephra correlates to the Guaje Pumice Bed or the Tsankawi Pumice bed); the bold incision rates represent our preferred correlation to the Guaje Pumice bed. Two incision rates are given for the late Pleistocene-Holocene. The higher rate (300 m/m.y.) uses the base of river gravel buried beneath Holocene alluvium under the modern Rio Ojo Caliente (36 ft; Wolf, 1996, unpublished consultant report for Ojo de Encantado subdivision along the southern Rio Ojo Caliente) and the time between the Qtoc6 base (median age of 143 ka) and the last glacial maximum (18 ka). The lower rate (210 m/m.y.) uses the modern river height and the time between 143 ka and the present.

rate of incision of 14-23 m/Ma is interpreted between 1.2-1.6 and 0.6 Ma, and a high rate of 140 m/Ma after 0.6 Ma (Fig. 13). The higher incision rate between 3.7 Ma and 1.2-1.6 Ma, compared to the two subsequent time intervals, may partly be an artifact of the longer measurement period. The high incision rate of 150 m/Ma between 640 ka and the present may be due to higher amplitude and frequencies of glacial-interglacial cycles during middle to late Pleistocene time, which would influence snow melt and periodically lead to increased discharges. Also, drainage capture in the upper Rio Grande (~440 ka, Machette et al., 2007) probably resulted in significant increases in discharge to this river in the Española Basin and probable increases in incision rates, leading to a lowering of base level for the Rio Chama and Rio Ojo Caliente after ~440 ka. The high, post-640 ka rate may also reflect regional Neogene high denudation and exhumation rates potentially due to mantle-driven uplift (Aslan et al., 2010; Karlstrom et al., 2010).

Base level fluctuations in White Rock Canyon likely influenced incision rates along the Rio Ojo Caliente. The head of this canyon is located ~27 km south of the mouth of the Rio Ojo Cali-

ente. Here, many base level rises and falls occurred in the Pleistocene due to landslides and damming by lava flows and ignimbrites (Reneau and Dethier, 1996). The lava flows are related to the Cerros del Rio volcanic field, generally date between 2.7-2.2 Ma (Thompson et al., 2006), and filled canyons incised as much as 180 m into the Miocene Santa Fe Group (Dethier and Fagenholz, 2007). A high-level tholeiite progressively dammed the Rio Grande between 2.48 and 2.33 Ma and created a lake with a shoreline elevation of ~1950 m (Dethier and Fagenholz, 2007), which would have extended into the lower Rio Ojo Caliente. Erosion in the northern Pajarito Plateau (northern edge shown in Fig. 1) was minimal between 2.4 and 1.6 Ma (Dethier and Fagenholz, 2007). Consequently, most of the incision along the lower Rio Ojo Caliente in the 3.7-1.6 Ma period likely occurred between 3.7 and 2.4 Ma. The two members of the Bandelier Tuff (1.62 Ma and 1.24 Ma) also dammed the river before they were breached. The latest lava dam occurred at 1.46 ± 0.06 Ma (Reneau and Dethier, 1996; basalt of Cochiti of Thompson et al., 2006, from which the age is cited). Landslides probably began as early as 0.5 Ma, with the largest landslides in the late Pleistocene. Movement along the La Bajada fault at the mouth of White Rock Canyon has created a 170-240 m escarpment and would have resulted in a cumulative drop in local base level sometime after 2.3-2.6 Ma (the age of the capping basaltic lavas; Thompson et al., 2006). In summary, tectonic and volcanic activity in White Rock Canyon influenced downstream base levels and, although likely attenuated, these base level effects may have extended to the Rio Ojo Caliente.

CONCLUSIONS

The most important conclusion of this work is that the basal gravel and strath of the 20-40 m terrace (Qtoc6) and its basin-wide equivalents are older than 103 ka and probably younger than 210 ka, with our preferred age being 130-160 ka. The base of this terrace likely formed during the glaciation associated with oxygen-isotope stage 6 or possibly the transition between stages 6 and 5. Its thick, sandy, locally derived fill was deposited shortly after the basal gravel and is similar to younger interglacial (Holocene) deposits elsewhere in the Española Basin. Following deposition of the basal gravel of Qtoc6 and at least 6-8 m of locally derived sand, downcutting occurred along the Rio Ojo Caliente followed by renewed aggradation -- as evident from stratigraphic relations at the La Madera travertine. Our data indicate a moderate rate of incision between 3.7 and 1.6 Ma (51-60 m/Ma), a low rate between 1.6 and 0.6 Ma (14-23 m/Ma), and a high rate after 0.6 Ma (150 m/Ma).

ACKNOWLEDGMENTS

Reviews by Dave Love, David Dethier, and Scott Aby significantly improved earlier drafts of this manuscript. Funding for geologic mapping along the Rio Ojo Caliente was provided by the STATEMAP component of the National Cooperative Geologic Mapping Program. Mark Mansell assisted with construction of Figures 1 through 4.

REFERENCES

Aby, S., Karlstrom, K., Koning, D., and Kempter, K., 2010, Preliminary geologic map of the Las Tablas quadrangle, Rio Arriba County, New Mexico: New Mexico Bureau of Geology and Mineral Resources, Open-file Geologic Map 200, 1:12,000.

Aslan, A., Karlstrom, K. E., Crossey, L. J., Kelley, S., Cole, R., Lazear, G., and Darling, A., 2010, Late Cenozoic evolution of the Colorado Rockies: Evidence for Neogene uplift and drainage integration, *in,* Morgan, L. A., and Quane, S. L., eds., Through the Generations: Geologic and Anthropogenic Field Excursions in the Rocky Mountains from Modern to Ancient: Geological Society of America Field Guide 18, p. 21-54.

Aster, R., MacCarthy, J., Heizler, M. T., Kelley, S. A., Karlstrom, K. E., Crossey, L. J., and Dueker, K., 2009, CREST Experiment Probes the Roots and Geologic History of the Colorado Rockies: Outcrop, v. 58, no. 1, p. 6-23.

Barker, F., 1958, Precambrian and Tertiary geology of Las Tablas Quadrangle, New Mexico: New Mexico Bureau of Mines and Mineral Resources Bulletin 45, 104 p.

Bingler, E.C., 1968, Geology and mineral resources of Rio Arriba County, New Mexico: New Mexico Bureau of Mines and Mineral Resources Bulletin 91, 158 p.

Bull, W.B., 1991, Climatic Geomorphology: Oxford, Oxford University Press, 326 p.

Connell, S.D., Hawley, J.W., and Love, D.W., 2005, Late Cenozoic drainage development in the southeastern basin and range of New Mexico, southeasternmost Arizona, and western Texas, *in,* Lucas, S.G., Morgan, G.S., and Zeigler, K.E., eds., New Mexico's Ice Ages, New Mexico Museum of Natural History and Science, Bulletin No. 28, p. 125-150.

Dethier, D.P., 2001, Pleistocene incision rates in the western United States calibrated using Lava Creek B tephra: Geology, v. 29, issue 9, p. 783-786.

Dethier, D.P., and McCoy, W.D., 1993, Aminostratigraphic relations and age of Quaternary deposits, northern Española Basin, New Mexico: Quaternary Research, v. 39, p. 222-230.

Dethier, D.P., and Reneau, S.L., 1995, Quaternary History of the western Española Basin, New Mexico: New Mexico Geological Society, 46th Field Conference Guidebook, p. 289-298.

Dethier, D.P., and Fagenholz, A.D., 2007, Late Pliocene deposition in Culebra Lake and Pleistocene erosion of lake sediment, northeastern Pajarito Plateau, New Mexico: N.M. Geological Society, 58th Field Conference Guidebook, p. 388-397.

Dethier, D.P., Harrington, C.D., and Aldrich, M.J., 1988, Late Cenozoic rates of erosion in the western Española basin, New Mexico: Evidence from geologic dating of erosion surfaces: Geological Society of America Bulletin, v. 100, p. 928-937.

Dethier, D.P., Harrington, C.D., Sarna-Wojcicki, A., and Meyer, C.E., 1990, Occurrence of the Lava Creek B tephra layer in the northwestern Española Basin, New Mexico: New Mexico Geology, v. 12, p. 77-82.

England, P., and Molnar, P., 1990, Surface uplift, uplift of rocks, and exhumation of rocks: Geology, v. 18, p. 1173–1177.

Gile, L.H., Hawley, J.W., and Grossman, R.B., 1981, Soils and geomorphology in the Basin and Range area of southern New Mexico – Guidebook to the Desert Project: New Mexico Bureau of Mines and Mineral Resources, Memoir 39, 222 p.

Gillam, M.L., 1998, Late Cenozoic geology and soils of the lower Animas River valley, Colorado and New Mexico [Ph.D. thesis]: Boulder, University of Colorado, 477 p.

Gillam, M.L., Moore, D.W., and Scott, G.R., 1984, Quaternary deposits and soils in the Durango area, southwestern Colorado, *in* Brew, D.C., ed., Geological Society of America, Rocky Mountain Section, 37th annual meeting, Durango, Colorado, Field trip guidebook: Durango, Colorado, Four Corners Geological Society and Fort Lewis College Department of Geology, p. 149–182.

Gutzler, D.S., 2004, Once and future climates in New Mexico and North America; the Icehouse and the Hothouse: "anti-analogues"?, *in,* Lucas, S.G., Morgan, G.S., and Zeigler, K.E., eds., New Mexico's Ice Ages: New Mexico Museum of Natural History and Science Bulletin No. 28, p. 277-280.

Hall, S.A., and Periman, R.D., 2007, Unusual Holocene alluvial record from Rio del Oso, Jemez Mountains, New Mexico: Paleoclimatic and archeological significance: New Mexico Geological Society, 58th Field Conference Guidebook, p. 459-468.

Hawley, J. W., 1995, Geology and ground water of the El Llano area: New Mexico Geological Society, 46th Field Conference Guidebook, p. 16-18.

Hawley, J.W., Bachman, G.O., Manley, K., 1976, Quaternary stratigraphy in the Basin and Range and Great Plains provinces, New Mexico and western Texas, in Mahaney, W.C., ed., Quaternary Stratigraphy of North American: Stroudsburg, PA, Dowden, Hutchinson, and Ross, Inc., p. 235-274.

Hillenbrand, C.D., Moreton, S.G., Caburlotto, A., Pudsey, C.J., Lucchi, R.G., Smellie, J.L., Benetti, S., Grobe, H., Hunt, J.B., and Larter, R.D., 2008, Volcanic time-markers for Marine Isotopic Stages 6 and 5 in Southern Ocean sediments and Antarctic ice cores: implications for tephra correlations between palaeoclimatic records: Quaternary Science Reviews, v. 27, p. 518-540.

Imbrie, J., Berger, A., Boyle, E.A., Clemens, S.C., Duffy, A., Howard, W.R., Kukla, G., Kutzbach, J., Martinson, D.G., McIntyre, A., Mix, A.C., Molfino, B., Morley, J.J., Peterson, L.C., Pisias, N.G., Prell, W.L., Raymo, M.E., Shackleton, M.J., and Toggweiller, J.R., 1993, On the structure and origin of major glaciation cycles, 2. The 100,000-year cycle: Paleoceanography, v. 8, no. 6, p. 699-735.

Izett, G.A., and Obradovich, J.D., 1994, $^{40}Ar/^{39}Ar$ age constraints for the Jaramillo Normal Subchron and Matuyama-Brunhes geomagnetic boundary: Journal of Geophysical Research, v. 99, p. 2925-2934.

Jansen, J.H.F., Kuijpers, A., and Troelstra, S.R., 1986, A mid-Brunhes climatic event: long-term changes in global atmosphere and ocean circulation: Science, v. 232, p. 619-622.

Johnpeer, G., D., Love, D.W., Hawley, J.W., Bobrow, D.J., Hemingway, M., and Reimers, R.F., 1985, El Llano and vicinity geotechnical study: unpublished report for the Office of Military Affairs, Santa Fe, NM.

Karlstrom, K.E., Crow, R., McIntosh, W., Peters, L., Pederson, J., Raucci, J., Crossey, L.J., Umhoefer, P., Dunbar, N., 2007, $^{40}Ar/^{39}Ar$ and field studies of Quaternary basalts in Grand Canyon and model for carving Grand Canyon: quantifying the interaction of river incision and normal faulting across the western edge of the Colorado Plateau: Geological Society of America Bulletin, v. 119, p. 1283-1312.

Karlstrom, K., Crow, R., Crossey, L., Coblentz, D., and Van Wijk, J., 2008, Model for tectonically driven incision of the younger than 6 Ma Grand Canyon: Geology, v. 36, no. 11, p. 835-838.

Karlstrom, K.E., Dueker, K., Aster, R. Maccarthy, J.K., Hansen, S., Crow, R, Kelley, S., Coblentz, D., 2010, CREST- Colorado Rockies Experiment and Seismic Transects: Time-space patterns of Neogene uplift and their correspondence to the Aspen anomaly: Geological Society of America Abstracts with Programs, v. 42, no. 5, p. 77.

Karner, D.B., Levine, J., Medeiros, B.P., and Muller, R.A., 2002, Correlating a stacked benthic $\delta^{18}O$ record: Paleoceanography, v. 17, no. 3, p. 2-1 to 2-12.

Kelley, V.C., 1978, Geology of the Española Basin, New Mexico: New Mexico Bureau of Mines and Mineral Resources, Geologic Map GM-48, scale 1:125,000.

Koning, D.J., 2003, revised 2005, Geologic map of the Chimayó 7.5-minute quadrangle, Rio Arriba and Santa Fe counties, New Mexico: New Mexico Bureau of Geology and Mineral Resources, Open-file Geologic Map OF-GM-71, scale 1:24,000.

Koning, D.J., 2004, Geologic map of the Lyden 7.5-minute quadrangle, Rio Arriba and Santa Fe counties, New Mexico: New Mexico Bureau of Geology and Mineral Resources, Open-file Geologic Map OF-GM-83, scale 1:24,000.

Koning, D.J., 2005, Quaternary terrace deposits along the lower Rio Chama and the Rio Chama-Rio Grande confluence: stratigraphic relations and possible displacement by the Santa Clara fault: N.M. Geological Society, 56th Field Conference Guidebook 56, p. 6-7.

Koning, D.J., and Maldonado, F., 2001, revised Oct-2003, Geologic map of the Horcado Ranch quadrangle, Santa Fe County, New Mexico: New Mexico Bureau of Mines and Mineral Resources, Open-file Geologic Map OF-GM-54, scale 1:24,000.

Koning, D.J., and Manley, K., 2003, revised December-2005, Geologic map of the San Juan Pueblo 7.5-minute quadrangle, Rio Arriba and Santa Fe counties, New Mexico: New Mexico Bureau of Geology and Mineral Resources, Open-file Geologic Map OF-GM-70, scale 1:24,000.

Koning, D.J., Nyman, M., Horning, R., Eppes, M., and Rogers, S., 2002, revised June-2005, Geology of the Cundiyo 7.5-min. quadrangle, Santa Fe County, New Mexico, New Mexico Bureau of Geology and Mineral Resources, Open-file Geologic Map OF-GM 56, scale 1:24,000.

Koning, D.J., May, S.J., Aby, S., Horning, R., 2004, Preliminary geologic map of the Medanales 7.5-minute quadrangle, Rio Arriba County, New Mexico: New Mexico Bureau of Geology and Mineral Resources, Open-file Geologic Map OF-GM-89, scale 1:24,000.

Koning, D.J., Skotnicki, S., Moore, J., and Kelley, S., 2005a, Geologic map of the Chili 7.5-minute quadrangle, Rio Arriba county, New Mexico: New Mexico Bureau of Geology and Mineral Resources, Open-file Geologic Map OF-GM-81, scale 1:24,000.

Koning, D.J., Karlstrom, K.E., May, J., Skotnicki, S.J., Horning, R., Newell, D., and Muehlberger, W.R., 2005b, Preliminary geologic map of the Ojo Caliente 7.5-minute quadrangle, Rio Arriba and Taos counties, New Mexico: New Mexico Bureau of Geology and Mineral Resources, Open-file geologic map 101, scale of 1:12,000.

Koning, D.J., Karlstrom, K., Salem, A., and Lombardi, C., 2007, Preliminary geologic map of the La Madera quadrangle, Rio Arriba County, New Mexico: New Mexico Bureau of Geology and Mineral Resources, Open-file geologic map 141, scale of 1:12,000.

Koning, D.J., McIntosh, W., and Dunbar, N., 2011a, Geology of southern Black Mesa, Española Basin, New Mexico: new stratigraphic age control and interpretations of the southern Embudo fault system of the Rio Grande rift: N.M. Geological Society, 62nd Field Conference Guidebook, p. 191-214.

Koning, D.J., Kempter, K.A., Peters, L., McIntosh, W.C., and May, S.J., 2011b, Miocene-Oligocene volcaniclastic deposits in the northern Abiquiu embayment and southern Tusas Mountains, New Mexico: N.M. Geological Society, 62nd Field Conference Guidebook, p. 251-274.

Kuehn, S.C., and Foit, F.F., 2006, Correlation of widespread Holocene and Pleistocene tephra layers from Newberry Volcano, Oregon, USA, using glass compositions and numerical analysis: Quaternary International, v. 148, p. 113-137.

Lanphere, M.A., Champion, D.E., Christiansen, R.L., Izett, G.A., and Obradovich, J.D., 2002, Revised ages for tuffs of the Yellowstone Plateau volcanic field: Assignment of the Huckleberry Ridge Tuff to a new geomagnetic polarity event: Geological Society of America Bulletin, v. 114, p. 559– 568.

Logsdon, M.J., 1981, A preliminary basin analysis of the El Rito Formation (Eocene), north-central New Mexico: Geological Society of America Bulletin, Part I., v. 92, p. 968-975.

Love, D.W., Reimers, R.F., Hawley, J.W., Johnpeer, G.D., and Bobrow, D.J., 1987, Summary of geotechnical investigations near Espanola, New Mexico, *in,* Menges, C., ed., Quaternary tectonics, landform evolution, soil chronolgies and glacial deposits – northern Rio Grande rift of New Mexico: Friends of the Pleistocene – Rocky Mountain Cell Field Trip Guidebook, p. 133-157.

Lucas, S.G., Koning, D.J., Heckert, A.B., Zeilger, K.E., Hunt, A.P., Owe, D.E., Maldonado, F., and Berglof, W.R., 2005, Rio Grande rift to the Colorado Plateau, First-Day Road log from Española to Abiquiu, Youngsville, Coyote, Gallina, and Ghost Ranch: New Mexico Geological Society, 56th Field Conference Guidebook, p. 1-38.

Machette, M.N., Marchetti, D.W., and Thompson, R.A., 2007, Ancient Lake Alamosa and the Pliocene to middle Pleistocene evolution of the Rio Grande, in Machette, M.N., Coates, M., and Johnson, M.L., eds., 2007 Rocky Mountain Section Friends of the Pleistocene Field Trip – Quaternary Geology of the San Luis Basin of Colorado and New Mexico, September 7-9, 2007: U.S. Geological Survey, Open-file Report 2007-1193, p. 157-167.

Maldonado, F., and Miggins, D., 2007, Geologic summary of the Abiquiu quadrangle, north-central New Mexico: N.M. Geological Society, 58th Field Conference Guidebook, p. 182-187.

Manley, K., 1979, Stratigraphy and structure of the Española basin, Rio Grande rift, New Mexico, *in* Riecker, R.E., ed., Rio Grande rift,: Tectonics and Magmatism: Washington, D.C., American Geophysical Union, p. 71-86.

Manley, K., 1981, Redefinition and description of the Los Pinos Formation of north-central New Mexico: Geological Society of America Bulletin, Part I, v. 92, p. 984-989.

Miller, J.P., and Wendorf, F., 1958, Alluvial chronology of the Tesuque Valley, New Mexico: Journal of Geology, v. 66, p. 177-194.

Minor, S.A., Hudson, M.R., Grauch, V.J.S., Sawyer, D.A., 2006, Structure of the Santo Domingo Basin and La Bajada constriction area, New Mexico, *in* Minor, S.A. (ed.), The Cerrillos Uplift, the La Bajada Constriction, and Hydrogeologic Framework of the Santo Domingo Basin, Rio Grande Rift, New Mexico: U.S. Geological Survey Professional Paper 1720, p. 91-120..

Morrison, R.B., 1991a, Introduction, *in,* Morrison, R.B., ed., Quaternary nonglacial geology, conterminous U.S.: Geological Society of America, The Geology of North America, v. K-2, p.1-12.

Morrison, R.B., 1991b, Quaternary geology of the southern Basin and Range province, *in,* Morrison, R.B., ed., Quaternary nonglacial geology, conterminous U.S.: Geological Society of America, The Geology of North America, v. K-2, p. 353-371.

Newell, D.L., Koning, D., Karlstrom, K.E., Crossey, L.J., and Dillon, M., 2004, Plio-Pleistocene incision history of the Rio Ojo Caliente, northern Española Basin, and overview of the Rio Grande system in northern New Mexico: N.M. Geological Society, 55th Field Conference Guidebook, p. 121-134.

Pazzaglia, F.J., 2005, River responses to ice age (Quaternary) climates in New Mexico, *in,* Lucas, S.G., Morgan, G.S., and Zeigler, K.E., eds., New Mexico's Ice Ages: New Mexico Museum of Natural History and Science Bulletin No. 28, p. 115-124.

Pazzaglia, F.J., and Kelley, S.A., 1998, Large-scale geomorphology and fission-track thermochronology in topographic and exhumation reconstructions of the southern Rocky Mountains: Rocky Mountain Geology, v. 33, p. 229–257.

Perkins, M., Nash, W., Brown, F., and Fleck, R., 1995, Fallout tuffs of Trapper Creek, Idaho- A record of Miocene explosive volcanism in the Snake River Plain volcanic province: Geological Society of America Bulletin, v. 107, p. 1484-1506.

Phillips E. H., Goff, F., Kyle, P.R., McIntosh, W.C., Dunbar, N.W., Gardner, J.N., 2007, The $^{40}Ar/^{39}Ar$ age constraints on the duration of resurgence at the Valles caldera, New Mexico: Journal of Geophysical Research, v. 112, B08201, 15 p.

Reilinger, R., and York, J.E., 1979, Relative crustal subsidence from leveling data in a seismically active part of the Rio Grande rift, New Mexico: Geology, v. 7, p. 139-143.

Reneau, S.L., and Dethier, D.P., 1996, Late Pleistocene landslide-dammed lakes along the Rio Grande, White Rock Canyon, New Mexico: Geological Society of America Bulletin, v. 108, p. 1492-1507.

Reneau, S.L., McDonald, E.V., Gardner, J.N., Kolbe, T.R., Carney, J.S., Watt, P.M., and Longmire, P.A., 1996a, Erosion and deposition on the Pajarito Plateau, New Mexico, and implications for geomorphic responses to late Quaternary climatic changes: N.M. Geological Society, 47th Field Conference Guidebook, p. 391-397.

Reneau, S., Gardner, J., and Forman, S., 1996b, New evidence for the age of the youngest eruptions in the Valles caldera: Geology, v. 24, p. 7-10.

Rogers, J.B., and Smartt, R.A., 1996, Climatic influences on Quaternary alluvial stratigraphy and terrace formation in the Jemez River valley, New Mexico: N.M. Geological Society, 47th Field Conference Guidebook, p. 347-356.

Sarna-Wojcicki, A.M., Morrison, S.D., Meyer, C.E., and Hillhouse, J.W., 1987, Correlation of upper Cenozoic tephra layers between sediments of the western United States and eastern Pacific Ocean and comparison with biostratigraphic and magnetostratigraphic age data: Geological Society of America Bulletin, v. 98, p. 207-223.

Sarnthein, M., Stremme, H.E., and Mangini, A., 1986, The Holstein interglaciation: time-stratigraphic position and correlation to stable isotope stratigraphy of deep-sea sediments: Quaternary Research, v. 26, p. 283-298.

Scott, G.R., and Marvin, R.F., 1985, Geologic map of the surficial deposits and basaltic rocks near the Rio Chama, Rio Arriba County, New Mexico: U.S. Geological Survey Miscellaneous Field Studies Map MF-1759.

Smith, H.T.U., 1938, Tertiary geology of the Abiquiu quadrangle, New Mexico: Journal of Geology, v. 46, p. 933-965.

Spell, T.L., Kyle, P.R., and Baker, J., 1996a, Geochronology and geochemistry of the Cerro Toledo Rhyolite: N.M. Geological Society, 47th Field Conference Guidebook, p. 263-268.

Spell, T., McDougall, I., and Doulgeris, A., 1996b, Cerro Toledo Rhyolite, Jemez volcanic field, New Mexico: Ar geochronology of eruptions between two caldera-forming events: Geological Society of America Bulletin, v. 108, p. 1549-1566.

Thompson, R.A., Sawyer, D.A., Hudson, M.R., Grauch, V.J.S., and McIntosh, W.C., 2006, Cenozoic volcanism of the La Bajada constriction area, New Mexico, *in,* Minor, S.A. (ed.), The Cerrillos Uplift, the La Bajada Constriction, and Hydrogeologic Framework of the Santo Domingo Basin, Rio Grande Rift, New Mexico: U.S. Geological Survey Professional Paper 1720, p. 43-60.

Toyoda, S., and Goff, F., 1996, Quartz in post-caldera rhyolites of Valles caldera, New Mexico: ESR finger printing and discussion of ESR ages: N.M. Geological Society, 47th Field Conference Guidebook, p. 303-309.

U.S. Geological Survey, 2011, USGS 08289000 Rio Ojo Caliente at La Madera, NM:< http://waterdata.usgs.gov/usa/nwis/uv?site_no=08289000> (accessed on April 21, 2011).

Wells, S.G., Kelson, K.I., and Menges, C.M., 1987, Quaternary evolution of fluvial systems in the northern Rio Grande rift, New Mexico and Colorado: Implications for entrenchment and integration of drainage systems, *in,* Menges, C., ed., Quaternary tectonics, landform evolution, soil chronologies and glacial deposits— Northern Rio Grande rift of New Mexico: Albuquerque, New Mexico, Friends of the Pleistocene–Rocky Mountain Cell Field Trip Guidebook, p. 55–69.

Williams, M.L., 1991, Heterogeneous deformation in a ductile fold-thrust belt: the Proterozoic tectonic history of the Tusas Mountains, New Mexico: Geological Society of America Bulletin, v.103, p.171-188

Winograd, I.J., Landwehr, J.M., Ludwig, K.R., Coplen, T.B., and Riggs, A.C., 1997, Duration and structure of the past four glaciations: Quaternary Research, v. 48, p. 141-154.

Zhang, P. Z., Molnar, P., and Downs, W. R., 2001, Increased sedimentation rates and grain sizes 2-4 Myr ago due to the influence of climate change on erosion rates: Nature, v. 410, no. 6831, p. 891-897.